INSTITUTE

FOR

AEROSPACE STUDIES
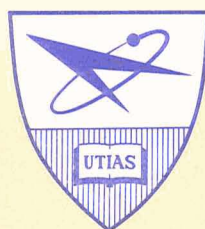
UNIVERSITY OF TORONTO

A PRELIMINARY MONTE-CARLO ANALYSIS OF THE REFLECTION OF AN

IMPLODING HEMISPHERICAL SHOCK WAVE SIMILAR TO

THAT GENERATED IN THE UTIAS IMPLOSION DRIVEN

HYPERVELOCITY LAUNCHER OR SHOCK TUBE

by

A. K. Macpherson

UTIAS

November, 1970.

UTIAS Report No. 152

ACKNOWLEDGEMENT

SUMMARY

The reflection of a hemispherical imploding shock wave in argon was studied in the region very close to the centre. Two aspects, which could not be studied by classical analysis near the centre, were the effect of a cold wall upon the reflection and multi-body collisional effects. The effect of the cold wall was examined using a Monte-Carlo technique and comparing the results obtained when the wall was treated as specularly reflective and diffuse reflective. It was found that a substantial difference occurred near the centre but it appeared that this effect would be rapidly damped. The multi-body collisional effects were studied using a modified form of molecular dynamics. The results show that reflection will occur before the imploding shock reaches the centre due to circumferential stresses in the shock. The result is a refraction type phenomenon, with reflected and transmitted waves.

TABLE OF CONTENTS   PAGE

NOTATION

c	velocity
m	mass
r	radius vector
$\dot{r}$	derivative of r with respect to time
t	time
v	velocity
x	distance from origin in x direction
y	distance from origin in y direction
z	distance from origin in z direction
A	collision cross section
M	molecular mass
N	number density
P	Pressure
R	Remainder
T	Time
V	Velocity
X	force in X direction
Y	force in Y direction
Z	force in Z direction

Greek Symbols

γ	ratio of specific heats
δ	incremental step
Δ	incremental or finite difference type step
σ	zero potential radius
ϕ	potential function

Subscripts

c	colliding
i	component
k	component
m	information transfer
A	Average or Argon
R_i	Relative
T	Tungsten

1. INTRODUCTION

In the analytic study of the performance of the UTIAS implosion-driven hypervelocity launcher [1 and 4], the assumption of spherical symmetry and the artificial viscosity techniques have been successful in studying the overall implosion phase. However, the assumptions are suspect when the collapse radius is reduced to a few mean free paths, such as would ideally occur if the imploding shock wave was absolutely symmetrical. The artificial viscosity technique produces shock structure by introducing an artificial pressure gradient which has the effect of giving the shock thickness even in inviscid flow. Towards the centre this thickness increases to unrealistically large values when an imploding shock is reflecting. Further, the difficulty arises in obtaining a realistic equation of state at the extreme densities expected at the centre. It was thus considered that a solution on a molecular level may provide a better insight into the physical processes involved.

As the solution of unsteady problems using the Boltzmann equation are relatively complex, Chu[5], the present study was undertaken using Monte-Carlo techniques. These methods have the limitation generally of only allowing a study of small regions of flow, but in the present case this restriction was not very important. The related problems of the collision of two planar shock waves and the reflection of a planar shock wave from a cold wall were first solved [6]. It was found that the results agreed with results from continuum theory. The assumptions of hard sphere molecules and binary collisions were made in these studies.

The effects of the cold wall upon a hemispherical implosion were studied using the technique developed by Bird [7]. In this analysis the assumptions of hard-sphere molecules and binary collisions were made. The shock was generated by a specularly reflecting piston and the wall was considered to be diffuse reflective. As the binary collision assumption probably breaks down near the centre, a hemisphere of radius of six mean free paths, in the undisturbed gas, was assumed to surround the centre. The hemisphere was considered to be specularly reflective. In order to investigate the effect of the diffuse reflective wall the calculation was repeated assuming that the wall was specularly reflective. These calculations are compared.

The restrictions imposed upon the flow by multi-body collisions were examined by a modified molecular dynamics type technique. Now the usual shock wave relations using perfect gas approximations can be used safely for dilute gases in the number density range $10^{16} - 10^{18}$ particles/ml and the pressure range $10^{-2} - 1$ atm. As pointed out by Devanathan and Bhatnagar [8] the following assumptions are made in the classical theories "(i) the statistics of the assembly is adequately represented by the single particle distribution function so that the particles can move freely except for occassional encounters with other particles (ii) the interaction between the particles is purely binary and takes place in a period of time much less than the duration of the mean flight time". It is also suggested that above 10 atmospheres marked discrepencies between theory and experiment occur.

In the present treatment a numerical study first is made of the generation of a planar shock wave in argon of initial number densities 0.73×10^{21} and 0.25×10^{22}, by a tungsten piston. The piston is driven into the gas at such a speed that a shock wave of Mach number 10 would be developed in a rarefied gas. This was performed for both initial number densities and the results presented. Similarly a piston velocity was chosen to develop a Mach number 20

shock and the experiment performed in the medium with the higher initial number density. The reflection of the imploding spherical shock wave is then simulated by a spherical piston imploding into a gas of initial number density 0.25×10^{22}.

2. EXPERIMENTAL TECHNIQUES

2.1 Bird Monte-Carlo Technique

Although Bird [7] has described his techique a number of times it appears worthwhile to give a brief account from a different viewpoint. Also the present author considers that a modification to the time advance parameter is necessary to produce a logically correct technique. The effect upon the overall result will probably be small except for some special problems.

2.11 An Alternative View of the Bird Monte-Carlo Technique

Consider the gasdynamic system under study to be made up of a series of comparatively small, but nevertheless macroscopic subsystems. These macroscopic bodies "behave approximately like closed systems over not too great periods of time. In fact, the particles which take part in the interaction of a subsystem with neighbouring parts of the system, are mainly those near its surface. Their number in comparison with the total number of particles in the subsystem quickly falls with an increase in size of the latter" [9]. Now generate a number of particles with random velocity components to represent the interacting or information transferring particles. These are assigned to various parts of the system in a random fashion. Consider each particle to have two roles, one as a typical subsystem particle and the other as an information transferring particle. Only these of all the particles in the system can transfer information. The remainder collide between themselves and take up typical average subsystem conditions dictated by the information particles being studied. As the time considered is short, particles can only transfer information from one subsystem to the next and usually the particles can only come from the right-hand half of one zone and the left-hand side of the next. In fact by choosing the time under consideration, ΔT_m, such that the fastest particle in the zone will not travel more than 0.4-0.5 of a zone width in ΔT_m, this can be assured.

While in their role of transferring information, all the particles from each half of a subsystem may be considered to be at the boundary so that any particle may collide with any other particle. Further, each subsystem is considered to be statistically independent of the next during time ΔT_m. Consider the first zone interface and select a pair of molecules at random. These are retained or rejected proportionally to their relative velocity. Having chosen a pair, a collision vector can be chosen at random as the colliding pair are assumed to be from any part of the field. The number of such collisions which can occur in time ΔT_m in a given zone is calculated upon the probable time for each collision chosen. The incremental time ΔT_i for a given collision can reasonably be chosen to be inversely proportional to the relative velocity of the pair, V_{Ri}, the collision cross-section, A, the number of colliding pairs of information particles, $N_c/2$, and the local number density, N. Therefore

$$\Delta T_m = \sum_{i=1}^{k} \Delta T_i = \sum_{i=1}^{k} \frac{1}{ANV_{Ri}N_c/2} \qquad (a)$$

2

after k collisions, that is inversely proportional to the swept volume and number of particles.

After this process has been repeated for each subsystem interface, the particles are allowed to take up their new positions and the cycle repeated.

2.12 Modified Time Advance Parameter

There arise two problems with Eq. a. Suppose ΔT_m = 2.0 and in one sub-system ΔT_1 = 1.3 and ΔT_2 = 1.1. If we only take $\Delta T_m = \Delta T_1$ a deficit of 0.7 in time exists, if $\Delta T_m = \Delta T_1 + \Delta T_2$ an excess of 0.4 in time is allowed. One possible solution is to consider that k must always be larger than 5, say, to keep the error relatively small. The second problem then arises where large density and temperature gradients exist in only part of the flow, such as through a shock wave. The value of a typical ΔT_k may be 50 times smaller behind a strong shock than in front so that to ensure that k = 5 in the pre-shock region, the post-shock k = 250. Thus during ΔT_m, on the average, every particle in each downstream subsystem will have collided at least once. This is unrealistic and contravenes restrictions upon statistical independence. Alternatively the subsystem may be kept large in width which will increase the number of particles in pre-shock zones and hence decrease ΔT_i there. Again, to maintain independence, large gradients of properties cannot be permitted in a closed subsystem. To keep gradients small the zone width must be fairly narrow with respect to the mean free path.

The solution proposed here is to calculate the probability of any collision occurring during a time δt. An estimate of the average collision time ΔT_A for a given subsystem is formed from Eq.a by substituting twice the average absolute value of the peculiar velocities of the subsystem, for V_{Ri}. A multiplication factor of two was chosen rather than the equilibrium value of $\sqrt{2}$ after running the program a number of times and examining the average collisional velocity through the shock. The average probability of a collision is taken to be $\delta t/T_A$. Thus when a stage is reached when the nth time step ΔT_k would make

$$\sum_{i=1}^{k} \Delta T_i > \Delta T_m$$

a random number R is chosen between 0 and 1.0 and if

$$\Delta T_m - \sum_{i=1}^{k-1} \Delta T_i / \Delta T_A < R$$

the collision was assumed to occur and T_m was taken to have elapsed exactly. If

$$R < \Delta T_m - \sum_{i=1}^{k-1} \Delta T_i / \Delta T_A \quad R$$

the collision was rejected and again ΔT_m was assumed to have elapsed. This settles the first problem raised. It also provides a solution to the second. If the time ΔT_m is adjusted for the dense regions, the rarefied upstream regions will all have $\Delta T_i \gg \Delta T_m$ so the above selection principle can be invoked. It should be particularly important in defining the front foot of the shock as small

errors from here may be transmitted downstream. In a problem with moving boundaries such as shock generation by a moving piston, the piston only transmits information about its motion while the particles are moving. Thus the sequence consists of an input of information from the piston and this is then transmitted to other parts of the system for a small time ΔT_m before further input is generated.

2.2 Molecular Dynamics Type Technique

The usual molecular-dynamics technique, [10], is to assign random positions and velocities to a small number of particles and to store these values in the computer. The molecules are then allowed to move in time steps of 10^{-14} sec by solving the set of Newtonian equations for the whole system of interacting particles. Interaction between particles is assumed to cease after some given radius from the given molecule typically 2.25σ, where is the zero potential radius in a Lennard-Jones potential. A predictor-corrector formula is used to increase the accuracy of the calculations.

As mentioned above, the present technique is similar to the molecular dynamics approach, but as it was developed independently it has a number of differences. The main aim of the differences is to decrease the computation time at the expense of accuracy. This is necessary to handle the large number of particles involved in generating a shock and even with the approximations used the computer time is very high. Further, it is not obvious that the standard molecular dynamics technique could calculate the high energy impacts occurring in the generation of a Mach 20 shock wave.

Consider a small prism of argon, typically a few hundred anstrogms (Å) long and 100 Å square, contained between two walls of tungsten. The walls are simulated by assuming the metal atoms are in two layers as shown in the two dimensional sketch in Fig. 1. A two-dimensional figure has been assumed for clarity although the actual simulation was in three dimensions. They are taken to be in a body centered cubic lattice with interparticle distance 3.16 Å. However, these atoms are assumed not to move relative to each other during the experiment. This was necessary as not only would the calculation of the vibration of each atom have required considerable extra computer time, but storage of the velocity and position coordinates would have been impossible with the core storage available in the computer used by the author. With fixed positions it was not necessary to store atom positions, assuming that a tungsten atom was situated at the point (0,0,0). This is equivalent to assuming that the wall is adiabatic. The argon atoms were simulated by choosing random positions and a Maxwellian velocity distribution. The number of particles were chosen to give the desired initial pressure assuming that the gas was a perfect gas. When inserting each new atom two restrictions were placed upon the position (i) the distance between the centre of the new particle and any existing particle must be less than $0.9\sigma_A$ (ii) no gas molecule must be closer to the wall than Dmin = σ_T, Fig. 1. Where σ_A and σ_T are the zero potential radii for argon-argon interaction and argon-tungsten interaction respectively. This was necessary as two molecules could be placed unrealistically close together so that even in time 10^{-14} sec the velocities would increase to unrealistic values. The periodic boundary condition was invoked on the lateral boundaries. That is, molecules which move out across BLU, Fig. 1, enter through BLL at the same x-coordinate. Thus it was necessary to keep all particles a distance - DMIN from BLU during the initial set up. In most parts of the region the velocities were

4

taken from a Maxwellian distribution appropriate to 300°K. However, near the
wall the Maxwellian velocity, was increased slightly due to particles coming
within the attractive field of the wall. This distance DGRAD, Fig. 1, was
taken to be 7.5 Å. The increase in velocity was such as to conserve energy of
the particle. It was realized that this was incorrect physically for, as has
been pointed out to the author by Dr. F. Goodman, the density, assuming perfect
gas properties, should obey a relationship like that proposed by Steele and
Halsey [11]. This was not followed as it was thought that the shock would be
developed sufficiently rapidly that the adsorption by the stationary wall would
not be significant. This was thought reasonable from the binary studies of shock
generation by Bird [7]. However the shock wave generation is slower and it
appears that it would have been better to allow some density variation. It does
not seem however that the shock properties would have been altered if an initial
density variation had been allowed.

The molecules are assumed to move for a short length of time Δt in a
force field which remains constant during this period. A similar assumption
was made by Lennard-Jones and Devonshire [12] and it was from this idea the
present work developed. Further, the force field is generated only by other
molecules within a sphere of given radius R, typically 7.5 Å. In the case of
molecules near BLU or BLL the sphere is assumed to extend to the other side of
the prism of gas. Thus the ith particle, shown encircled in Fig. 1, will be
assumed to move while all the surrounding molecules remain stationary. Having
found the new velocity and position for the ith particle it is returned to its
original position and the new values stored. The i + 1th particle is then ex-
amined and so on until the whole field is covered. The particles then take
up their new positions and velocities and the cycle is repeated. In practice
the method was to order the particles in increasing x and to calculate the
interaction between the ith and i + 1th particle. The required force values
for the i + 1th particle were then stored as the negative of that for the ith
particle. This saved double calculation. Wall effects were allowed for by con-
sidering the interaction of the gas atom with the closest sixteen tungsten atoms.
Originally the technique by Jackson and French [13] of assuming that outside a
given distance from the wall the wall effects should be integrated to infinity,
was tried. It was found that very large fluctuations in wall pressure occurred.
This may be due to the nature of the wall model used here.

The motion of the ith molecule, with mass M and position vector $\hat{r}_i$
and velocity vector $\hat{v}_i$ at time t_1, was calculated by the Taylor series expansions

$$\hat{r}_i(t) = \hat{r}_i(t_1) + \dot{\hat{r}}_i(t_1)(t-t_1) + \ddot{\hat{r}}_i(t_1)(t-t_1)^2/2! +$$
$$\dddot{\hat{r}}_i(t_1)(t-t_1)^3/3! \tag{1}$$

$$\hat{v}_i(t) = \hat{v}_i(t_1) + \ddot{\hat{r}}_i(t-t_1) + \dddot{\hat{r}}_i(t-t_1)^2/2! \tag{2}$$

where

$$\ddot{\hat{r}}_i = \frac{1}{M}\frac{\partial\phi}{\partial r_i} \text{ and } \dddot{\hat{r}}_i = \frac{1}{M}\frac{\partial^2\phi}{\partial r_i^2}V_i$$

where ϕ is the potential function at r_i.

In the present case ϕ is generated by the surrounding atoms at r_j distance r_{ij} from r_i.

$$\overset{\wedge}{\ddot{r}}_i = \sum_{\substack{j \\ j \neq l}} \frac{1}{M} \frac{\partial \phi_{ij}}{\partial r_{ij}} \cdot \frac{\hat{r}_i - \hat{r}_j}{r_{ij}} \qquad (3)$$

$$\overset{\wedge}{\dddot{r}}_i = \sum_{\substack{j \\ j \neq l}} \frac{1}{M} \frac{\partial^2 \phi_{ij}}{\partial r_{ij}^2} \frac{\hat{r}_i - \hat{r}_j}{r_{ij}} V_r \qquad (4)$$

where V_r is the relative velocity of the two particles. Thus by letting $(t-t_1)$ be small, i.e., $\Delta t = 10^{-14}$ sec for a Mach 10 shock wave, the positions and velocities could be found. Even using the third derivative it was found that in time Δt particles could move unrealistically close together. In the next time step they would then be driven apart with such high velocities that the whole system would eventually become unstable. Thus when two particles would in a given time step became less than 2.15 Å apart it was assumed in a side calculation that these two particles collided on their own. The time step was reduced by a factor of 10 and ten small steps were taken. When the new positions and velocities were found the equivalent value of $\ddot{r}_i$ was calculated which would take the particles from their initial velocities to the final velocities. This value of $\ddot{r}_i$ was then used in the normal calculation assuming all relevant particles were interacting. This device was only needed during the early stages of establishing the Mach 10 shock although it was needed throughout the whole of the Mach 20 wave generation. The time step Δt was reduced to 0.4×10^{-14} sec in the latter case.

In an earlier treatment, [14], similar assumptions were made except that instead of using a Taylor series expansion it was assumed that the change in potential energy in time Δt was converted into a change in kinetic energy, i.e.,

$$\Delta \phi = \sum \frac{\partial \phi_{ij}}{\partial r_i} (t-t_1) V_{ij}(t_1) \qquad (5)$$

$$V_i(t) = \text{sqrt} (V_i(t_1)^2 - 2\Delta\phi \cdot V_i(t_1)(t-t_1)/M) \qquad (6)$$

However, further study of individual collisions showed that it was possible under some conditions for an unrealistically close approach between molecules to occur before repulsion. An example of this occurs when two molecules are chasing each other with the rearmost molecule having the higher velocity and overtaking the front one. This gave high velocities and hence high temperature peaks. In the present technique the $\ddot{r}_i$ term provided early warning of the approach of the second molecule. Although it was thought that the present technique would allow larger time steps that 10^{-14} sec this did not occur. Rather, the time steps in [14] should have been smaller.

3. EXPERIMENTAL DETAILS

3.1 Cold Wall Study

Physical details of simulated gaseous regions.

The initial piston radius was approximately 45 mean free paths (λ) of the undisturbed gas, for the cold wall study as shown in Fig.2. The cells were produced from j hemispherical shells Z_{ij}, initially 1.2λ in width reducing as the piston moved in to 0.5λ. After this the number of shells were reduced to keep the width approximately constant in width. In shells where sufficient atoms were present to allow 10 atoms in the smallest cell, four cells Z_{ij}, $(i = 1 - 4)$ were formed. The cell Z_{1j} was formed by the volume between the azimuthal angles (measured from the x axis) 0 and 4.5^O, Z_{2j} between 4.5^O and 9°, Z_{3j} between 9° and 13.5^O and Z_{4j} between 13.5^O and 90° of the radius vector when swept through all polar angles. On all other occasions only 3 zones were formed where the azimuthal angle moved in steps of 30°. The centre of the sphere was surrounded by a sphere of radius 6λ. Initially the atoms were distributed throughout the whole volume with a Maxwellian velocity distribution. While in the information transferring mode an assumption of spherical symmetry was made with each cell so that the azimuthal (θ) and polar (ϕ) angles could be ignored. Thus each particle's velocity was transformed to a set of axes with the radius vector (r) as the x_1 axis, the x_2 axis as $r\theta$ and the x_3 axis as $SQRT(x^2 + y^2).\phi$. After the collisional process was complete for time ΔT_m the velocities were transformed back to the original axes for the purpose of moving the particles. A total of 4,000 particles were used to simulate the process, which had an initial number density of 2×10^{18}.

3.2 Dense Gas Study

An experiment consisted of setting the molecules up, as described above, to simulate a temperature of 273^OK (T_o) and a kinetic pressure as required (P_o), then allowing them to collide for 0.55×10^{-13} sec or fifty-five cycles. From initial studies it appeared that this would be sufficient time to allow largest fluctuations due to the expanding gas to be damped. It was realized that the gas was not in a steady state by this time but it appeared that sufficient computer time to achieve an equilibrium state could not be reasonably obtained. This would amount to several hours before the experiment commenced. However these fluctuations do not appear to seriously affect the general results. After the initial settling time the piston was moved at the velocity necessary to generate the desired Mach number assuming binary collisions [6]. In order to prevent excessively violent collisions between wall atoms and gas atoms, the potential was calculated, assuming that the wall had moved through half the distance it would during the time interval Δt. In all cases the Lennard-Jones potential

$$\phi = t \left((\sigma/r)^{12} - (\sigma/r)^6 \right) \tag{7}$$

For argon-argon interaction $t = 1.71 \times 10^{-14}$ ergs

$$\sigma = 3.42 \overset{o}{A}$$

for argon-tungsten interaction $\quad t = 1.78 \times 10^{-13}$ ergs

$$\sigma = 3.07 \text{ Å}$$

where r = interparticle distance.

In the imploding shock wave study the piston was assumed to be constructed of argon atoms closely spaced in two rows. As the piston imploded the spacing was reduced as with fixed spacing it would appear to the gas atoms that the piston was rotating circumferentially.

4. RESULTS

4.1 Effects of a Cold Wall on an Imploding Shock Wave

The origin of coordinates has been taken to be the surface of the sphere surrounding the origin, that is in the present case 6λ from the hemisphere's centre. The variation of temperature pressure and density through the shock wave with a specularly reflecting wall is shown in Fig. 3 at a time $0.002762/V_m$ sec. after the piston started moving. This is the same as the spherically symmetric case which will be used for comparison. A pronounced peak is formed in the temperature profile at the shock front. The reciprocal slope shock thickness when compared with the planar case [6], shows that the shock waves here are approximately twice as thick as in the planar case. The corresponding case with a cold wall for the region where only 3 cells could be formed in each shell is shown in Fig's. 4, 5 and 6. These give the results for the region where only 3 cells could be formed and represent cells Z_{1j}, Z_{2j} and Z_{3j} as designated in Fig. 2. Only the front foot of the shock is shown here and by comparison with Fig. 3 it can be seen that the temperature profile lags behind the result for the spherically symmetric case. However the profile with the cold wall is steeper than in the spherical case. Where four cells per shell were formed the situation is vastly different, Fig. 7. Zone 1 are the cells closest to the wall (at Z_{1j}, Fig.2) and Zone 4 are the cells Z_{4j}. The pressure and density profiles in zone 1 show that the pressure and density are much higher close to the piston than in the symmetric case. The temperature is lower but it can be seen that the most significant feature is that the shock front is retarded. This retardation is seen in the temperature and pressure profiles in zone 2. However, the pressure and density in zones 2, 3 and 4 are approximately that in the symmetric case. The retardation of the temperature is not seen in zone 3 but the value is lower than for the symmetric case. Although it was felt that insufficient data was available to be confident that statistical fluctuations had been eliminated, the temperature profile in zone 4 appears to have a similar peak as in Fig.3. The value at the top of the peak and at the piston also correspond. Thus the picture which evolves is of a shock which has been retarded by the cold wall and is slightly elliptical. However the values of density or pressure a short distance from the wall are not greatly affected.

Generally the most interesting region is the part of the flow around the origin during the reflection process. The pressure and temperature profiles for the simulated spherically symmetric case are shown in Fig.8. A steady increase in both temperature and pressure are found except for an overshoot in the temperature for a short time. The same case with a cold wall is shown in Fig's. 9 and 10 showing pressure and temperature profiles at approximately the same time as in Fig.8. Zone 1 is the cells closest to the wall, Z_{ij} in Fig. 2

8

and zone 3 is Z_{3j}, where the conditions were such that only 3 cells per shell could be formed. Zone 3 behaved very much like the spherically symmetric case although in this case the overshoot was in pressure rather than temperature. However, the final results were very similar. In zone 1 the shock was initially slightly retarded and both pressure and temperature were a little less than in zone 3. The significant feature was the presence of a thermal boundary layer near the centre which also reduced the pressure. This was most marked at times T_4, T_5 and T_6. It appeared that as the density built up at the centre that this vanished. Neither the temperature nor the pressure in zone 1 reached those in zone 3. However, the reflected shock front did not lag behind in zone 1 at time T_7 significantly.

The initial stage of reflection for the diffuse reflective wall is shown in Fig. 11. The temperature profile is the slowest in development and the generation of the reflecting shock can be seen in all three profiles. This lag in the development of the temperature profile is contrary to that found for the reflection of a planar shock wave [6], where it was found that the shock temperature profile was the first to form.

The final results produced, Fig's. 12 to 16, were at a time $0.0046/V_m$ sec. after the motion started. In the case of spherical symmetry, Fig. 12, fairly smooth curves were obtained for pressure and velocity profiles. A kink is shown in the temperature profile as the results indicated one. This probably is not meaningful and may be due to statistical scatter. The shock front position is well defined by the density ratio. In this case the density has started falling at the origin due to expansion waves generated by the outward motion of the shock. The pressure reciprocal shock thickness shows that the shock is about three times as thick as in the planar case. The temperature profile is not so well defined, but is at least as much as three times thicker than the planar case. The results for the corresponding cold wall case are shown in Fig's. 13 to 15. Figure 13 represents those cells closest to the wall, Z_{1j}, Fig. 14 the Z_{2j} cells and Fig. 15 the centre cells, Z_{3j}. The profiles for zone Z_{3j} are very similar to those for the spherical case. The cells close to the wall show a weaker reflected shock as the peak values of pressure, temperature and density are lower in Fig. 15 than in Fig. 13. In addition, expansion waves have travelled faster here than in the centre zone and the profiles of temperature, pressure and density all show a decrease at the origin. However, the velocity of the shock front is the same in both cases. Although not of direct concern to the present study, the results for the diffuse wall case near the piston face are shown in Fig. 16 at a time $0.004624/V_m$ sec. The cold wall has produced a very strong shock wave in both the density and temperature profiles. A steady gradient in temperature is seen away from the wall and a thermal boundary layer is well established.

Thus the overall picture here is that both the incoming and reflected waves will move at the same speed and hence retain a hemispherical shape. The region near the wall will, have a weaker shock in terms of temperature, density and pressure.

4.2 Imploding Spherical Shock in a Dense Gas

The results are presented in the form of temperature, pressure and density calculated in narrow zones. A fixed number of twenty-one divisions were used at all piston positions, so that at times when the total distance was small the results were obtained on a finer grid. The kinetic temperature

9

was calculated as the sum of the squares of the peculiar velocities, [12]and is referred to as T_k the kinetic temperature. This combines with the density to give the kinetic pressure P_k. The virial of Clausius [16] is used to calculate the total pressure P_T. This gives

$$3 \; P/\rho = \sum mc^2 + \sum (xX + yY + zZ) \tag{8}$$

where x, y, z are the position coordinates of the molecule and X, Y, Z are the forces acting upon the molecule. In the case of a potential which is dependent upon the distance between the molecules this reduces to

$$3 \; P/\rho = \sum mc^2 + \sum rF(r) \tag{9}$$

where $F(r)$ is the force between the particles distant r apart. Provided the sign of $F(r)$ is taken as positive or negative according to whether it is a repulsive or attractive force the relation (9) may be used for mixed signed forces as in the present case. The forces between the wall molecules and the gas molecules must be included in X, Y, Z for the zones near to the wall. As it was convenient to perform the summations before the zones were established, it was assumed that no contribution to the summation was made by particles on the left side of a given zone and that the total of the interacting forces on the right side were added to the given zone. The pressures were non-dimensionalized with respect to the kinetic pressure initially established. Similarly, density and temperature were non-dimensionalized with respect to the initial conditions. The results are shown as block diagrams with a line sketched through the results for identification. No attempt has been made to use a curve fitting technique as generally the accuracy obtainable from one "experimental" run is not sufficient to make such an exercise worthwhile. Thus the block diagrams should be studied although in some regions of the undisturbed flow this is not possible. However, even in these regions the fluctuations obtained are of interest.

Using a piston velocity of 0.29 x 10^5 cm/sec, a tungsten surface, initial number density of 0.245 x 10^{22} and initial distance between walls of 204 Å, the density ratio, kinetic temperature ratio, kinetic and total pressure ratios are shown for three times in Fig. 17. Assuming binary collision theory the start of test conditions would be 100 atmospheres, 21 mean free paths between walls, Mach number 10 shock wave and resultant test times of approximately 4, 9, 10 mean time between collisions (τ). The shock equilibrium values of density, temperature and pressure ratios using binary-collision theory for a Mach number 10, $\gamma = 1.67$ ideal gas would be 3.93, 31.7, 124.6 respectively. The time to develop these values after the piston commences moving has been shown, [7], to be about one mean collision time in the undisturbed gas. In Fig. 17a after 4τ the binary collision results have not been achieved although the equilibrium temperature profile with a peak value of about 10 at approximately two mean free paths from the piston has been established. It appears that the equilibrium values are obtained between 4 and 5τ and the established profile is shown in Fig. 17b at time 9τ. The total pressure is approximately the same as the binary collision theory, the density ratio is about 2-1/2 times greater and the temperature ratio less than 10. The slow rise to equilibrium values is due to the large proportion of pressure due to inter-molecular forces, the kinetic equilibrium being established much quicker. A maximum temperature ratio of

18 was found at a time 0.5τ, but this damped fairly rapidly as the density increased. The final result of physical significance is shown in Fig. 17c at time 10τ. In this, the physical adsorption at the stationary wall has altered the initial conditions so that further results could not be obtained. A very large positive pressure peak is found at a distance from the wall equal to the bottom of the potential well of the Lennard-Jones potential between tungsten and argon. The pressure closer to the wall becomes negative. Due to the large gradients in properties probably the last results which can be confidently used are those in Fig. 17b. As indicated by the long development times the Mach number of the wave is much less than 10, although the mass velocity of the fluid behind the shock is the same as the binary collision results. Approximate contours of constant mass velocity are shown in Fig. 18. It should be emphasized that this figure is generally produced from only one set of results and thus the position of the curves are probably only accurate to 4 Å. The results in Fig's. 2 and 3 were repeated for varying run times with different initial random particle positions and velocities. Figure 17a is the average of 6 results although Fig's. 17b and 17c are produced from only one test. Generally the scatter between runs was small and less than would be suggested by theories such as those by Smoluchowski, [15].

Longitudinal velocity distribution profiles, integrated with respect to both lateral velocity distributions, were obtained for each zone at the completion of the test. The results are shown in Fig. 19 plotted with a probability or Poisson ordinate. With this ordinate a Maxwellian distribution will appear as a straight line through the 50% ordinate and 0.0 abscissa points.

These results may be compared with those in [7] using a binary collision assumption. It is found that a similar result is obtained. The zone near the piston is Maxwellian with a small standard deviation. On moving through the shock the average value becomes negative [7]. The average became positive as in the present case the piston moves from the positive x coordinate towards the origin and a second Maxwellian is formed on the positive side. This bump is seen clearly in the results by Bird [7]. In front of the shock a Maxwellian of larger standard deviation is found. Thus using an entirely different technique from Bird and a dense gas where inter-molecular forces are important, the same velocity distribution profiles have been obtained. This gave added confidence in the present results.

From these results it appeared that the potential of the wall could dominate the shock structure or at least substantially modify it. Thus an experiment was simulated by enclosing the gas between two pistons constructed of argon atoms in a body centered-cubic lattice as before, with an inter-molecular spacing of 1.5 Å. The results of Fig. 20 are shown at time 9τ after the piston commenced moving, and can be compared with Fig. 17b. The effects of the stationary wall upon the gas at the left hand side are seen to be much less than before, however, the shock properties are within expected statistical scatter. This strongly suggests that the results are a function of the gas inter-molecular potential only. Using a 360/65 IBM computer the computation time to obtain Fig's. 17b and 20 were 8 hours; to continue to obtain Fig. 17c required an additional 4 hours. The time varies by the cube of the density approximately and as the shock develops the cycle time becomes much greater. Thus only a limited number of cases could be studied due to the high computer time requirements.

A study was performed using a piston velocity of 0.586×10^5 cms/sec, which would generate a Mach number 20 shock wave assuming binary collision theory.

The values of density ratio, temperature ratio and pressure ratio would then be 3.98, 126, 501. Figure 21 shows the results with initial number density 0.245 x 10^{22}. Again the pressure ratio reaches the classical result, the density ratio is approximately 2-1/2 times the classical result and the temperature ratio is just less than 30. The integrated longitudinal velocity distributions are shown in Fig. 22 and although the standard deviation is greater the same trend is found.

It would be desirable to check the method by generating a shock wave in a gas with initial pressure equal to 1 atmosphere. However it appears that this would require about 30 hours computer time and in addition only about three or four mean free paths of undisturbed gas could be simulated. One result which goes some way towards such a proof is given at the end of the path. Using a tungsten piston and an initial number density of 0.737 x 10^{21} a simulated experiment was performed. The distance between the walls was 680 Å or 22 mean free paths of the undisturbed gas. After the piston has been in motion for about 10τ a well developed shock wave is formed as in Fig.23. Again the pressure ratio is approximately that obtained from binary collision theory, the temperature ratio is again slightly less than 10. However the density ratio now is over 30 and is about three times that obtained with the higher initial number density. This means that the actual density was the same at the piston face in both cases. This suggests the conclusion that the temperature ratio is limited by a type "space charge" due to the high initial density. Once a certain initial density is exceeded a given piston speed will only generate a limited molecular velocity. Thus if the pressure is determined by the piston forces then the density must accommodate the difference. An examination of the integrated longitudinal velocity distributions gave the results in Fig. 24. Again the same pattern was reproduced through the shock wave.

The longitudinal force upon the walls for the case of .245 x 10^{22} initial number density is plotted in Fig. 25 as a function of time. The fine fluctuating lines indicate the instantaneous variation and the heavy line shows the average force on the stationary wall. Similar fluctuations about the mean were found on the moving piston but only the mean result can be shown. Certainly some of the early time fluctuations are due to the initial expansion process although as can be seen the first 0.55 x 10^{-12} sec have not been shown nor used in calculating the average. Even large peaks were found on both walls at times $4 - 5 \times 10^{-12}$ sec after initial settling period. Some of these effects may be reduced if a non-rigid wall had been used.

The reflection of a spherically-symmetrical, imploding shock wave was studied by considering a sector of gas with included angle approximately 11° in both orthogonal circumferential directions. The radial boundaries consisted of dense argon surfaces as described above with intermolecular spacing 1.5 Å. The centre boundary was a sphere 2 mean free paths in radius i.e., 19. 4 Å. The initial outer piston radius was 620 Å, the initial number density 0.245 x 10^{22} and the piston velocity was .293 x 10^{6} cm/sec. Again the periodic boundary condition was used along both circumferential directions. The conditions after the piston had moved for about 11τ is shown in Fig. 26a. The density and temperature ratios are about the same as for the planar case although the temperature profile has a plateau rather than a sharp peak. The kinetic pressure does not dip at the piston surface as the temperature gradient at the piston is less than in the planar case. The total pressure is substantially lower than in the planar case due to the reducing area not producing as high a resistance as in the planar case. The results at a time 22τ are shown in Fig. 26b. At this stage all

12

variables except the temperature have risen very substantially. A curious front plateau appears in the density ratio although from one set of results it may not be significant. At a time 0.6×10^{-12} sec later, Fig. 26c, a reflected pressure wave can be seen to have developed about 20 Å from the piston. The pressure ratio rises from 600 at the piston to about 1000 at the point where reflection occurred. Comparing Fig's. 26b and 26c it can be seen that the pressure pulse also reflects in the density profile. The kinetic temperature profile is not so peaked in Fig. 26c as in Fig. 26b. The effect of this reflected wave striking the imploding piston was observed in the results at a time $.1162 \times 10^{-10}$ sec. A pressure ratio of 0.9×10^6 was formed near the piston in a very narrow region. In an experiment the piston would be sufficiently far from the reflection point that this event would not arise, thus the results at later times, Fig. 26d, probably have no physical significance. The high-temperature and pressure peaks, Fig. 26d, towards the centre are the result of the intense reflected wave moving very rapidly through the dense gas till it reached the relatively rarefied gas near the centre. The molecules at the front of the shock were propelled at high velocities by this wave and gave apparently high temperatures and pressures. The pressures and density profiles show the reinforced wave moving rapidly towards the centre.

One test was performed with an initial density of three atmospheres and the results are shown in Fig. 27. The piston had been in motion for about 0.6τ, and it can be seen that apparently the binary collision temperature, pressure and density ratios have been established as if the shock wave was plane. However as this was for the spherical case and the time to equilibrium found by Bird of 1.0τ had not been reached the results are not conclusive. However it can be seen that the temperature limit found previously has not occurred in this case and a ratio of 30 has been achieved. It should be mentioned that these results required about 20 hours of computer time before the experiment was terminated.

4.3 Application of Results to the Hypervelocity Launcher

Due to requirements of computational simplicity neither of the studies are directly applicable to the Hypervelocity Launcher. As only binary collisions were allowed in the cold wall study the density is much lower than occurs in the experiment. However it would appear that the conclusion that the cold wall will not substantially alter the shock shape in the dense hot gas can be drawn. The application of the results from the dense gas study cannot be so readily extrapolated to the experiment. The numerical study was set up in Argon in order to avoid the complexities due to polyatomic molecules. This simplification could be very important as the gas in the experiment is at least a mixture of H, O, H_2, O_2, H_2O, OH. Once a very strong imploding shock passes through such a mixture the ionization problems would need consideration. Even in Argon if realistic shock Mach numbers of say 100 to 200 were used ionization effects would require consideration. Thus in the study here the Mach numbers were restricted so that ionization effects would not be significant. Again to reduce the computer time an initial gas density was chosen such that the mean free path was the same order as the interparticle distance. This density was about 100 atmospheres whereas the launcher initial pressure is about 30 atmospheres. Studies at the lower pressure would increase the computer time by about an order of magnitude. Finally, in this study, the shock wave was driven by a constant velocity piston whereas in the launcher the piston is much further from the centre and the shock is driven at the centre by the decreasing spherical area. Thus the present results cannot be directly compared with either experiment or other theory. However the two most significant conclusions which can be drawn are (a) that an imploding shock in a dense gas can get very close to the centre

and (b) refraction of the shock wave will occur before the centre is reached. It would not appear that sufficient correlation exists between this study and the experiment to try to estimate the distance from the centre that refraction will occur. However if the Mach number of the shock reaches 100 then refraction may occur a measurable distance from the centre. Some allowance for the above effects would need to be made before a reasonable extrapolation could be expected. On the other hand the present results could serve to stimulate continuum studies to obtain refraction effects such as found here.

5. CONCLUSIONS

The effect of a cold wall upon an imploding hemispherical shock has been found to decrease the pressure, temperature and density in the region near the wall. However, this is a localized effect as the velocity of the reflected shock, including that within the wall region, is virtually unaltered. It would be expected that some distance from the centre the effect would be negligible.

At an initial pressure between 3 atmospheres and 30 atmospheres it appears that the temperature ratio developed by a Mach number 10 shock wave becomes limited to a maximum of 8. This value is maintained for initial pressures up to over 100 atmospheres and is approximately one quarter of the binary collision result. The nominally Mach number 20 shock wave also gave approximately one quarter of the binary collision result. The pressure ratio obtained is approximately that calculated by binary collision theory and the density ratio is adjusted to match the temperature and pressure ratios. At high Mach numbers with initial number densities of $.245 \times 10^{22}$ the pressure again is that calculated by binary collision theory, the density ratio is the same as for Mach number 10 and the temperature ratio is adjusted to match these. The integrated longitudinal velocity distribution function through all the planar shock waves studied agreed generally with the results found for binary collision theory.

A spherically symmetrical imploding shock wave does not reach the centre before reflection. With an initial number density of 0.245×10^{22} the wave reflects about 120 Å from the centre of the sphere. The process is similar to shock wave refraction and a transmitted wave continues to the centre and a reflected wave outward. Possibly as the transmitted wave strengthens refraction may be possible again.

REFERENCES

1. Sevray, P.A.L.   Performance Analysis of UTIAS Implosion-Driven Hypervelocity Launcher, UTIAS T.N. #121, Jan, 1968.

2. Flagg, R. F.   An Optimization Study of the UTIAS Implosion
   Mitchell, G. P.   Driven Hypervelocity Launcher MK II. UTIAS T.N. #130, Dec, 1968.

3. Brode, H. L.   Theoretical Description of the Performance of the UTIAS Hypervelocity Launcher, Proceedings, Second International Colloquium on the Gasdynamics of Explosions and Reactive Systems, Astronautica Acta (to be published).

4. Glass, I. I.   Implosion-Driven Shock Tubes, Proceedings Seventh
   Poinssot, J. C.   International Shock Tube Symposium, University of Toronto Press, 1970.

5. Chu, C. K.   Kinetic-Theoretic Description of Shock Wave Formation II, Phys. Fluids, $\underline{8}$, No.8, p.1450, 1965.

6. Macpherson, A. K.   Shock Collision at a Molecular Level, J. F. M., $\underline{39}$, pt. 4, p.849, 1969.

7. Bird, G. A.   The Velocity Distribution Function within a Shock Wave, J.F.M., $\underline{30}$, pt. 3, p.479, 1967.

8. Devanathan, C.   Transport Processes in Dense Gases. Proc. Roy.
   Bhatnagar, P. L.   Soc., A.309, p.245, 1969.

9. Landau, L. D.   Statistical Physics. Pergamon, London, p.6, 1958.
   Lifshitz, E. M.

10. Rahman, A.   Correlations in the Motion of Atoms in Liquid Argon, Phys. Rev., $\underline{136}$, p.405, 1964.

11. Steele, W. A.   The Interaction of Gas Molecules with Capillary
    Halsey, G. D.   and Crystal Lattice Surfaces, J. Phys. Chem., $\underline{59}$, p.57, 1955.

12. Lennard-Jones, J.E.   Critical Phenomena in Gases – I. Proc. Roy. Soc.,
    Devonshire, A.F. $\underline{A163}$, p.54, 1937.

13. Jackson, D. P.   High Energy Scattering of Inert Gases from Well
    French, J. B.   Characterized Surfaces – II Theoretical. Rarefied Gasdynamics Symposium, Vol. II, p.1119, Academic Press, New York, 1969.

14. Macpherson, A. K.   A Collisional Treatment of the Reflection of an Imploding Hemispherical Shock Wave. Proceedings of the 7th International Shock Tube Symposium (in press)

15. Lee, J. F.   Statistical Thermodynamics, Addison-Wesley, p. 298,
  Sears, F. W.   1963.
  Turcotte, D. L.
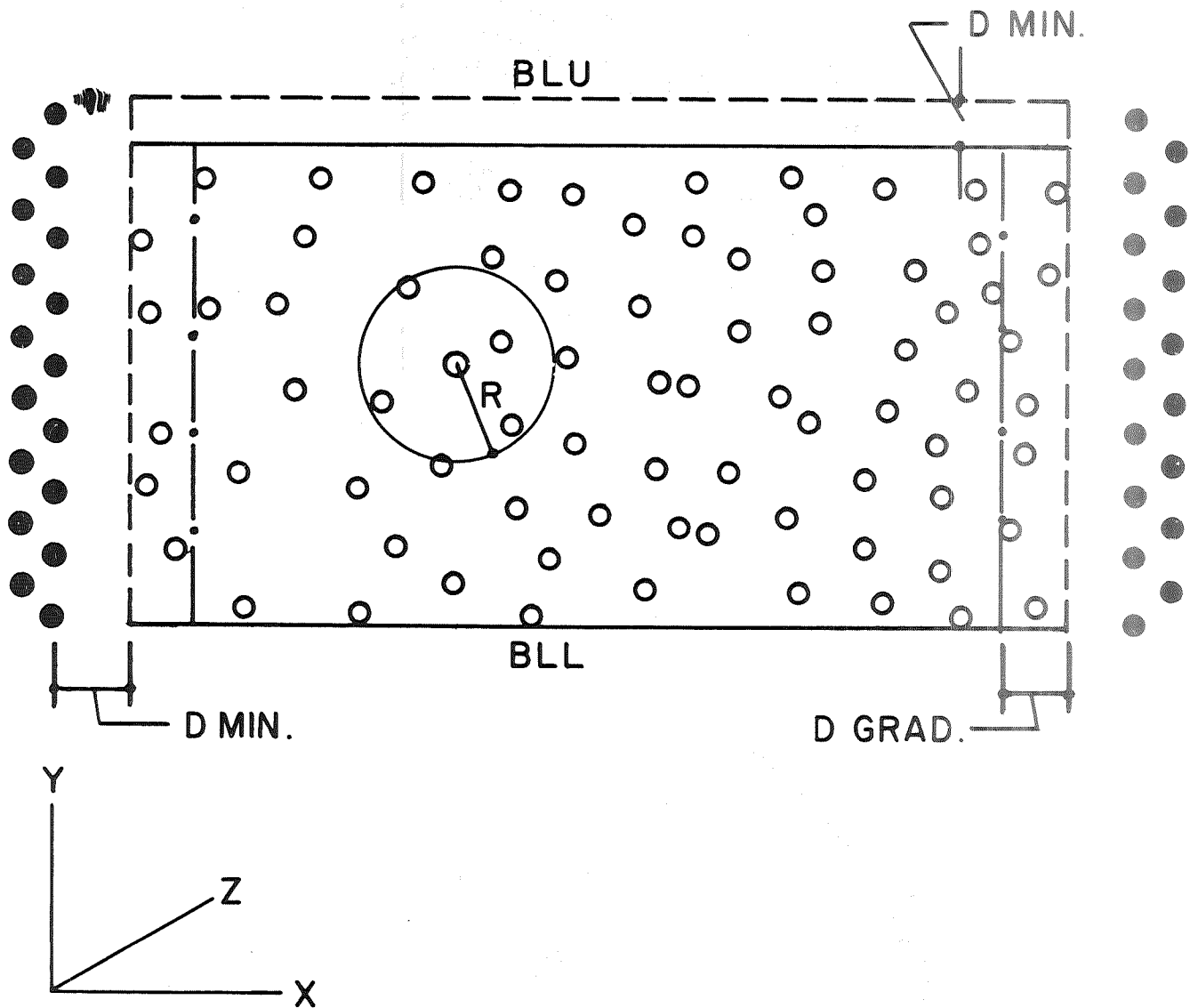
Fig.1 Two-dimensional view of Argon gas molecules (o) and
Tungsten wall molecules (•) used in studying planar
shock waves. Actual simulation was in three dimen-
sions

Z_{i6} Z_{i4} Z_{i2} Z_{i1} Z_{i3} Z_{i5} Z_{i7} Z_{ij}

12 M.F.P.
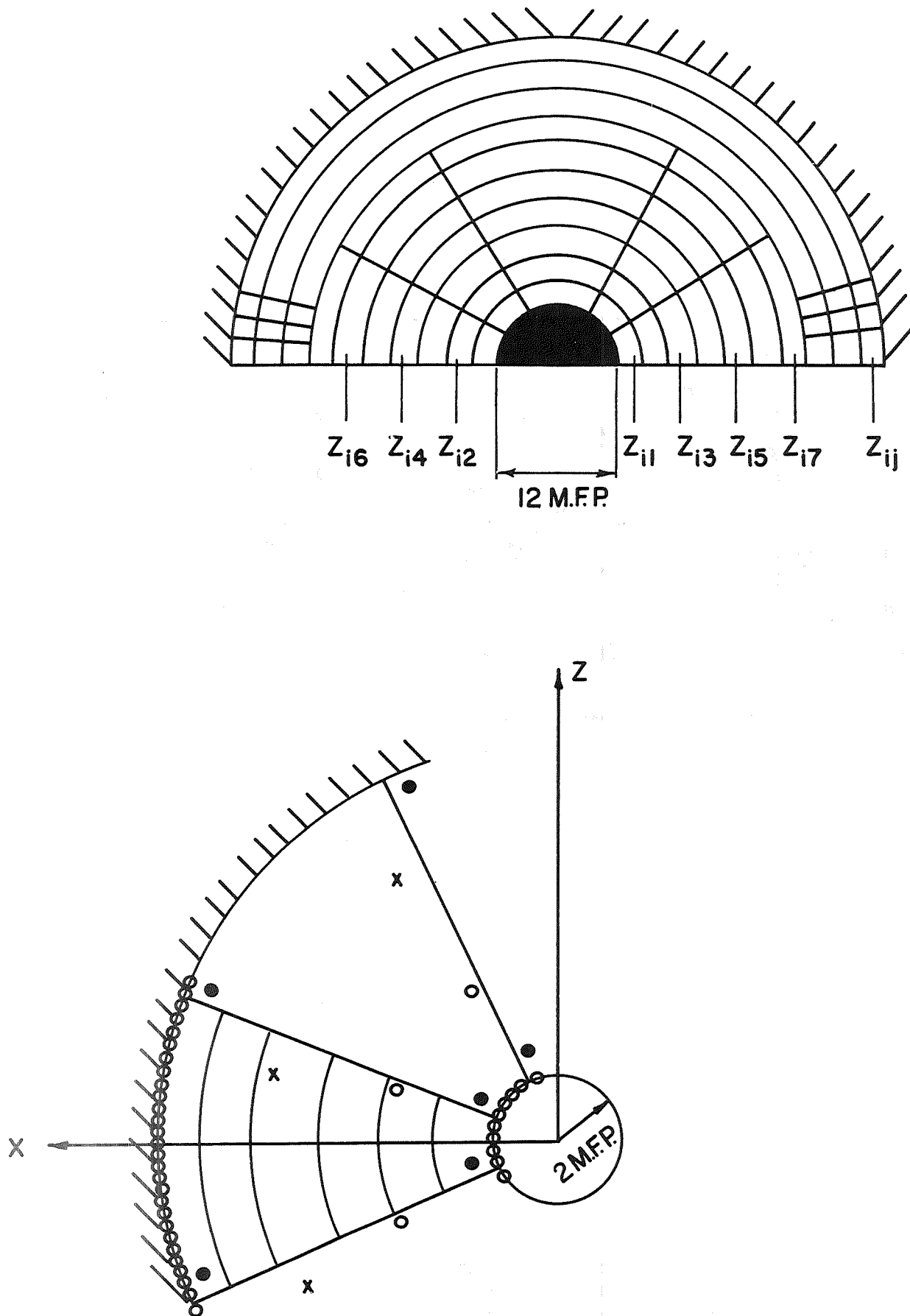
FIGURE 2:   PERIODIC BOUNDARY CONDITION AND CELL ARRANGEMENT FOR
IMPLOSION IN DENSE GAS
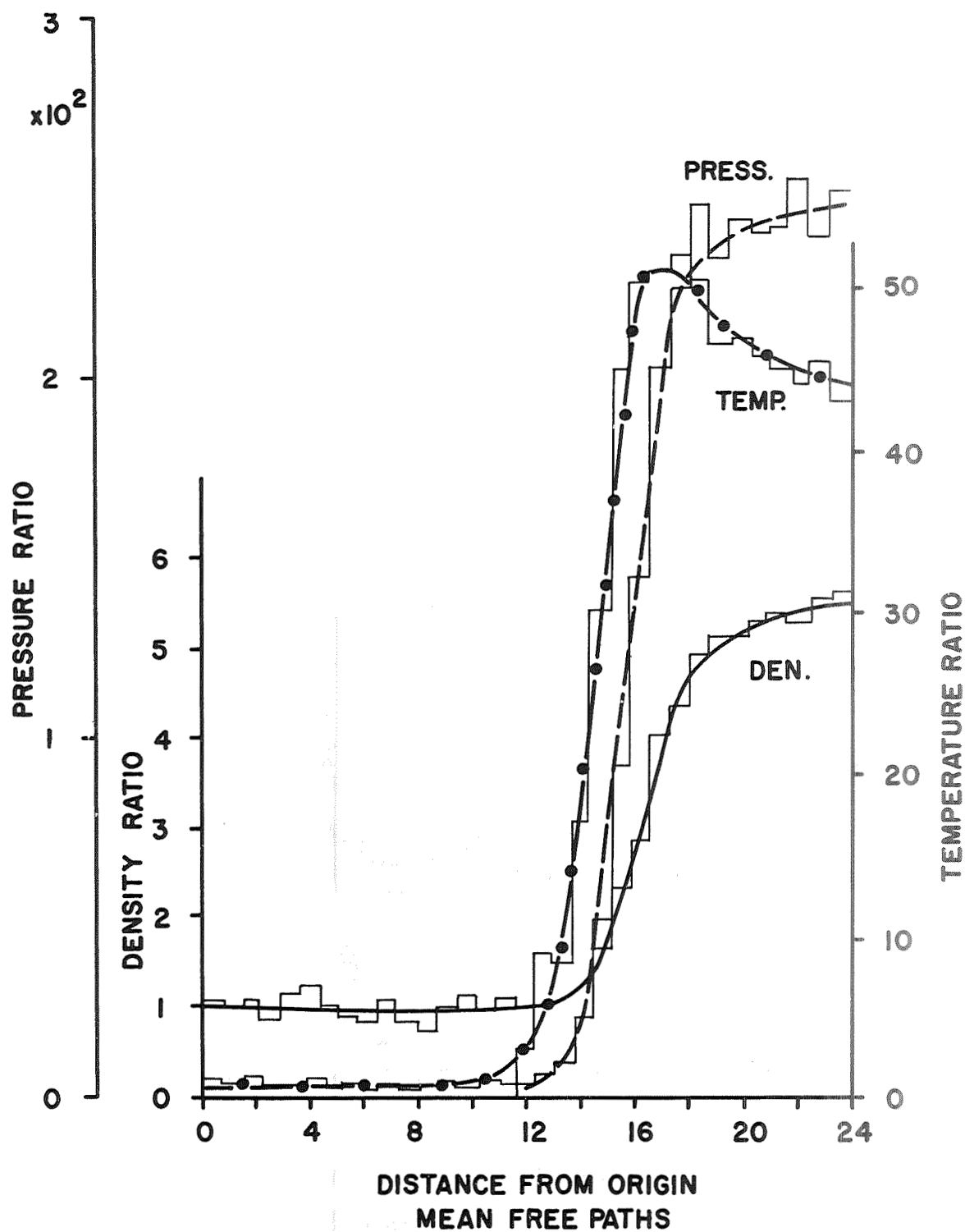
FIGURE 3: DENSITY, PRESSURE AND TEMPERATURE PROFILES OF GAS DRIVEN BY AN IMPLODING HEMISPHERICAL PISTON AT TIME 0.002762/Vm SEC. AFTER PISTON COMMENCED MOVING SPECULARLY REFLECTING WALL. ORIGIN OF CO-ORDINATES 6 MEAN FREE PATHS FROM CENTRE
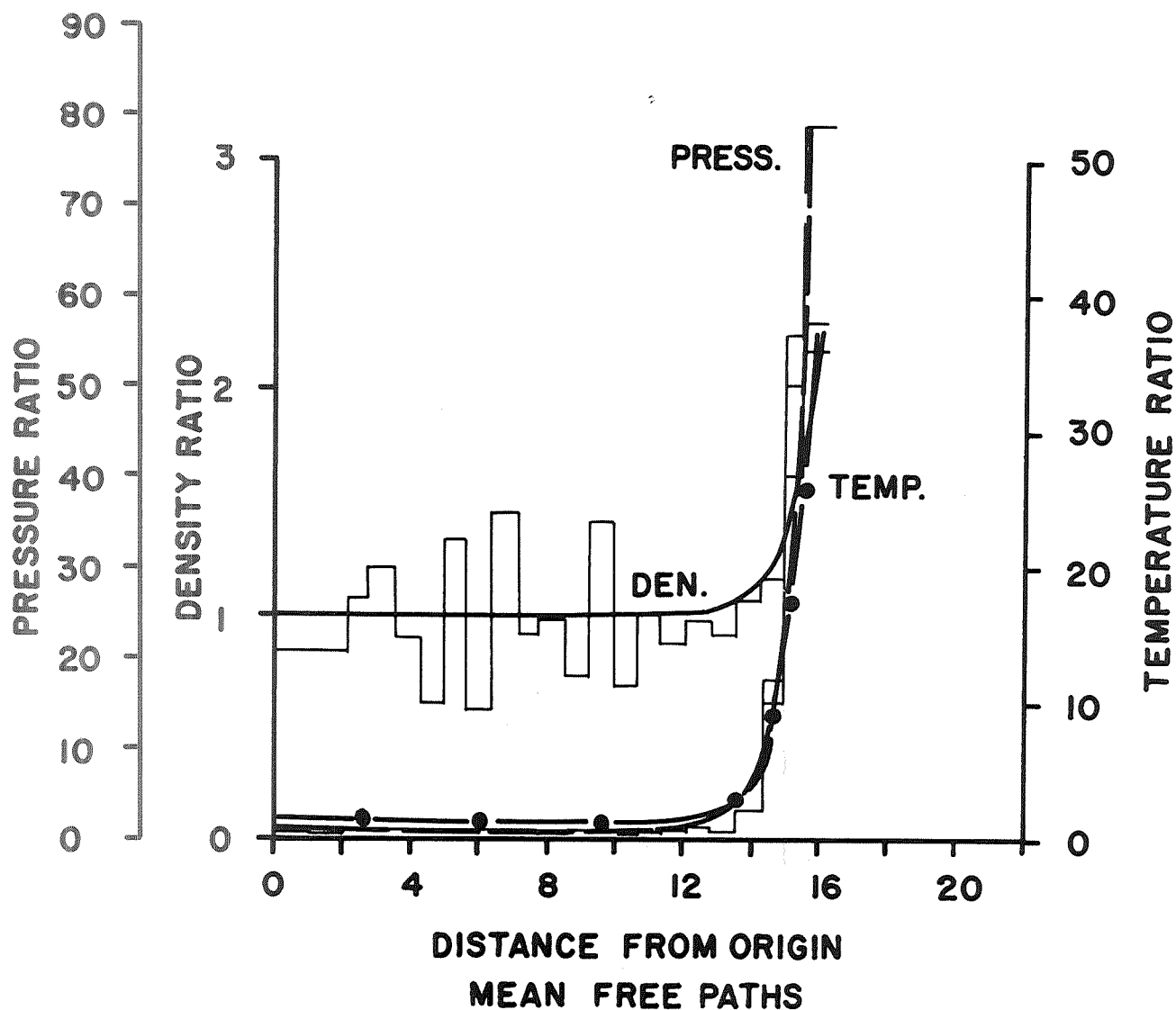
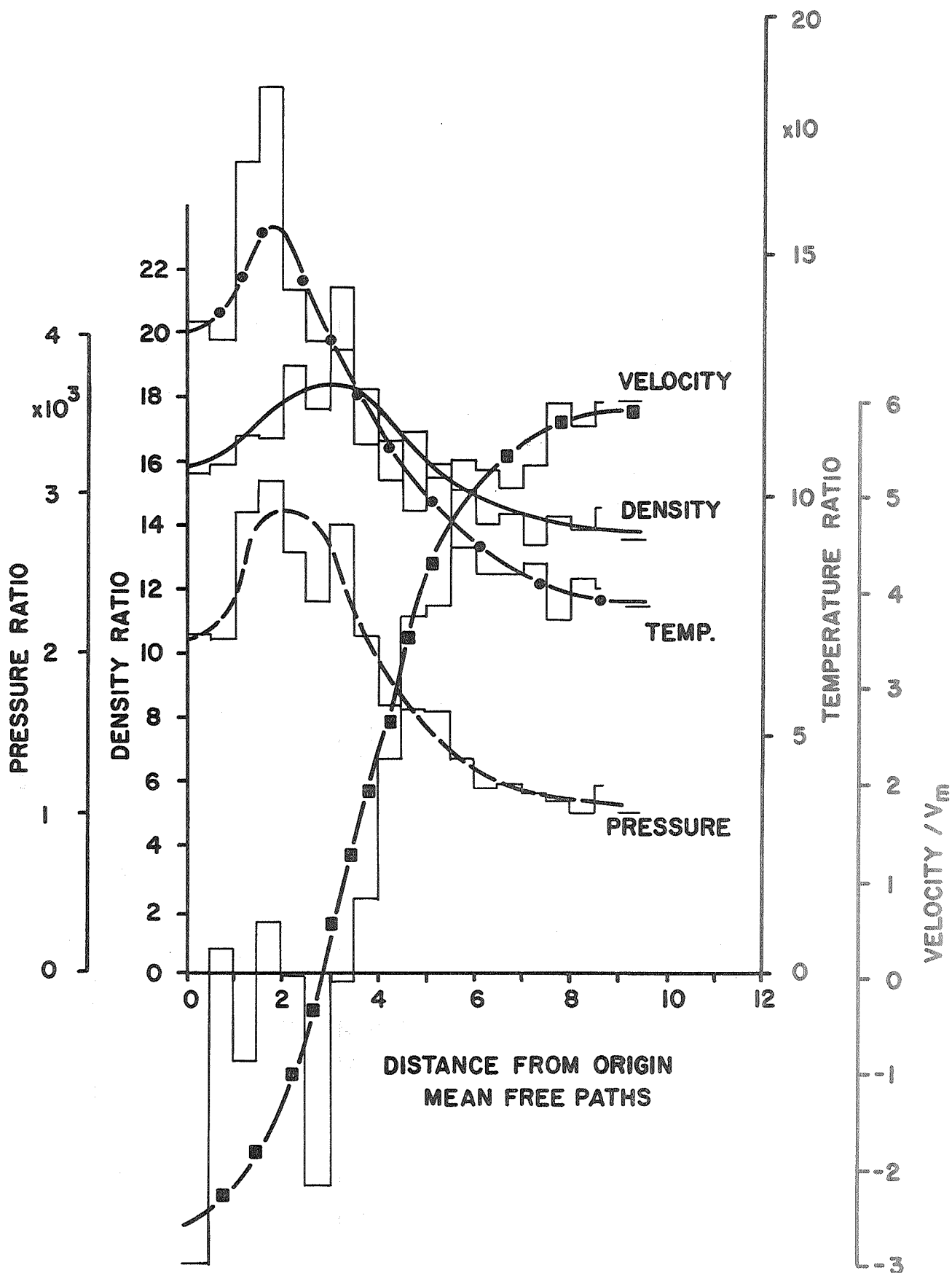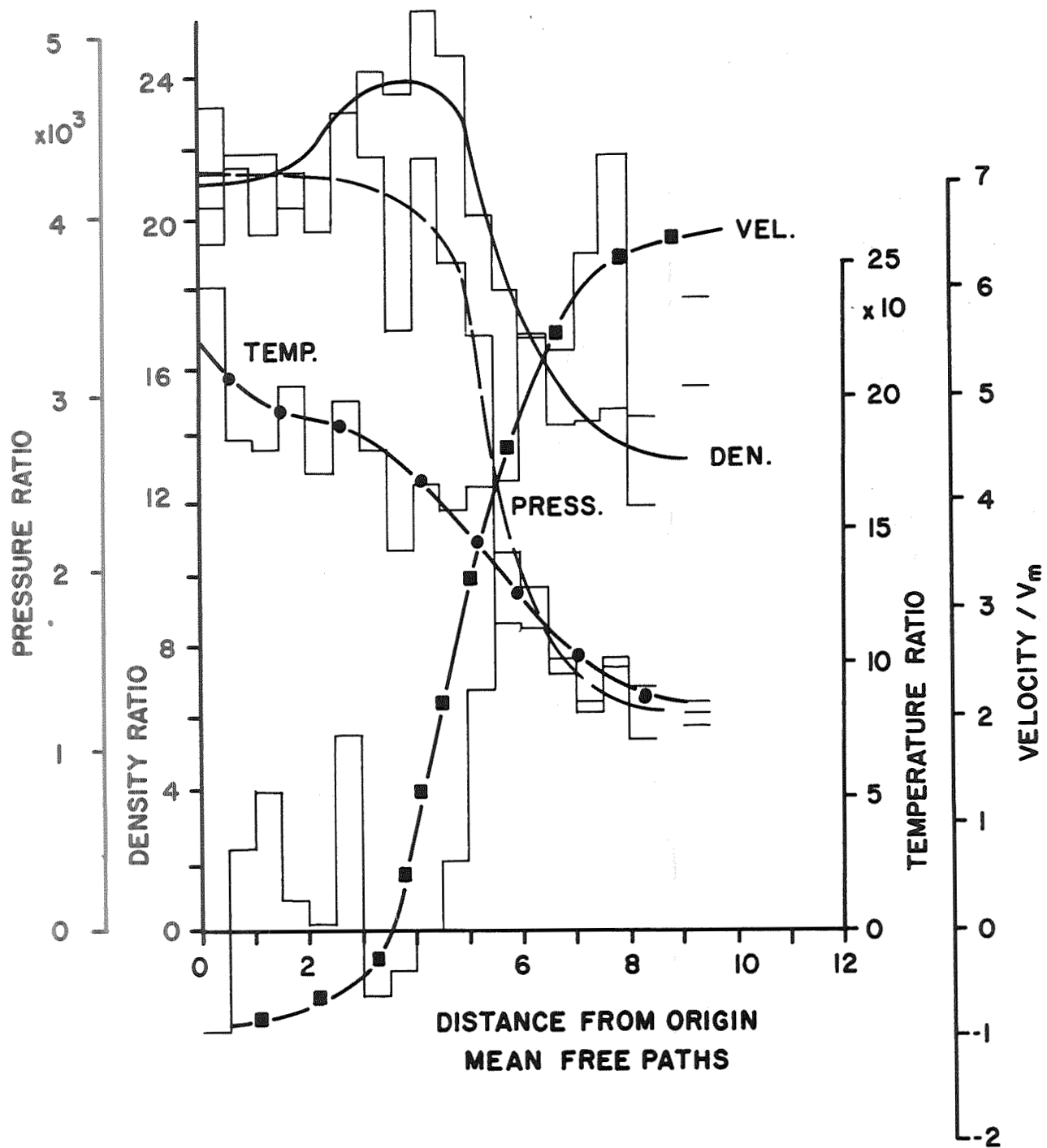FIGURE 4: DENSITY, PRESSURE AND TEMPERATURE PROFILES OF IMPLODING SHOCK
WAVE AT TIME 0.002726/Vm SEC AFTER PISTON COMMENCED MOVING.
DIFFUSE REFLECTIVE WALL. REGIONS WHERE 3 CELLS PER SHELL
FORMED. ORIGIN OF CO-ORDINATES 6 MEAN FREE PATHS FROM CENTRE,
CELLS IN Z_{1j} NEAR THE WALL
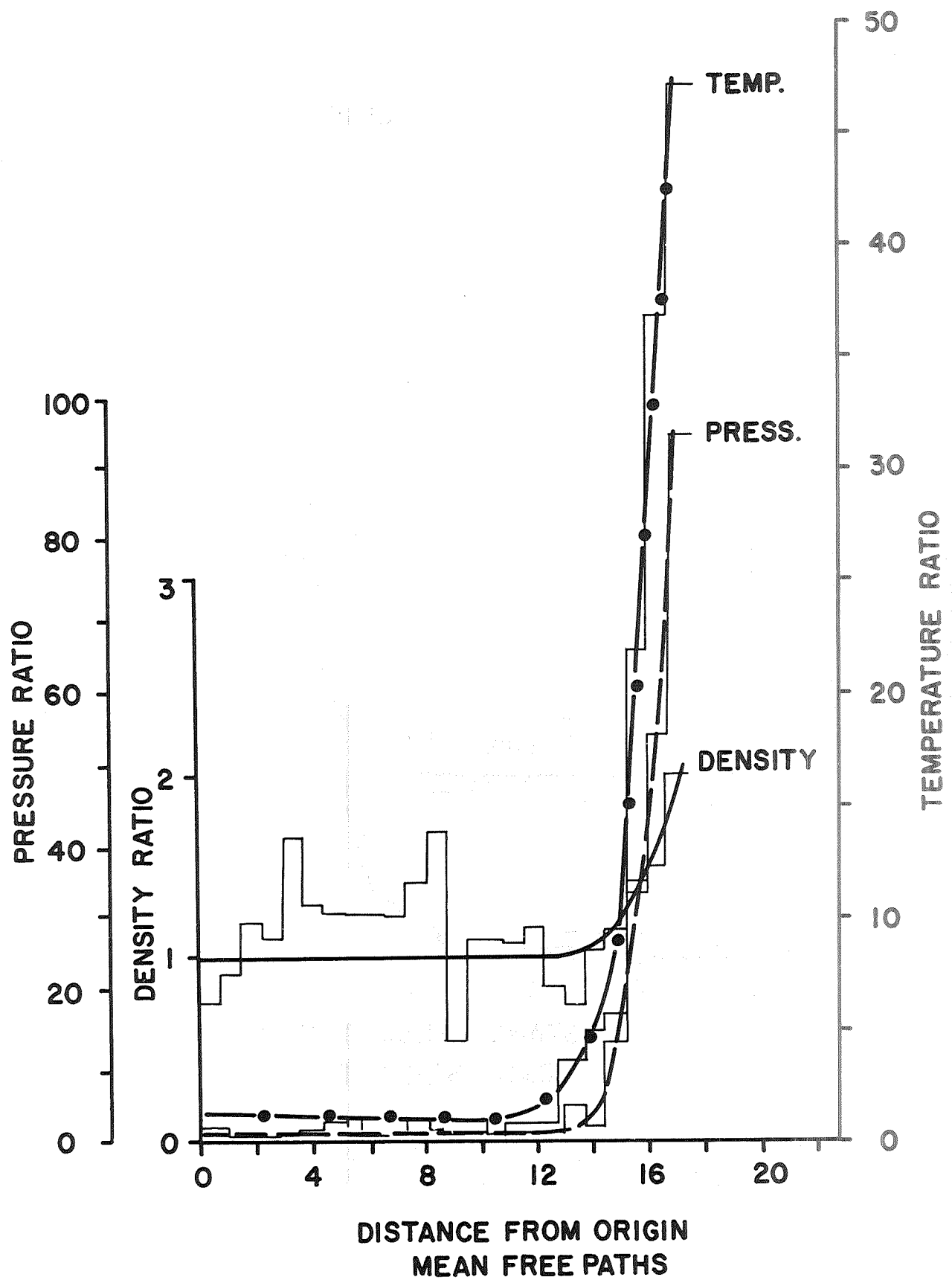
FIGURE 5:   DENSITY, PRESSURE AND TEMPERATURE PROFILES OF IMPLODING
SHOCK WAVE AS IN FIG.4 FOR CELLS Z_{2j}, SEE FIG.2
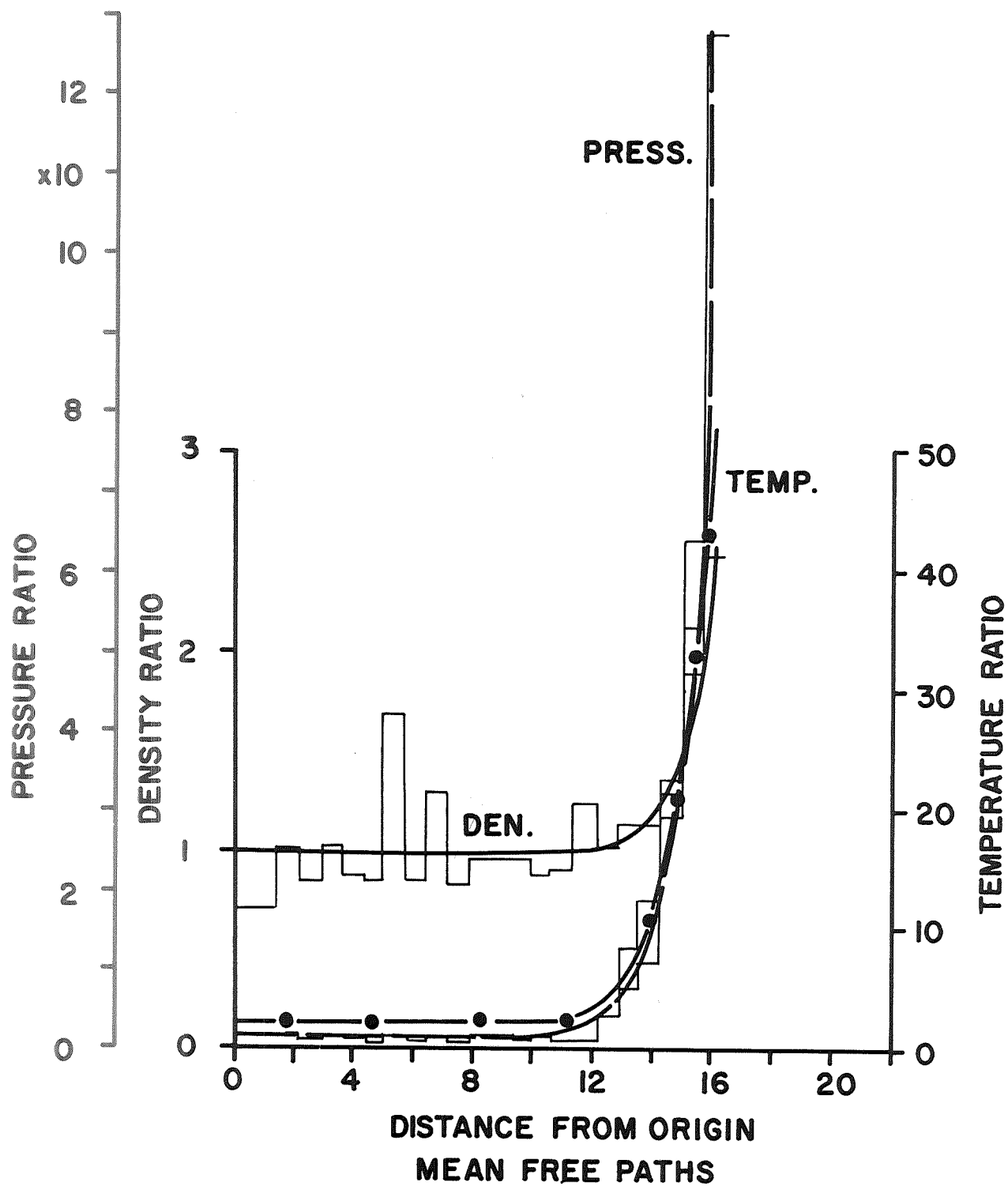
FIGURE 6: DENSITY, PRESSURE AND TEMPERATURE PROFILES OF IMPLODING SHOCK WAVE AS IN FIG.4 FOR CELLS Z_{3j}, SEE FIG.2.
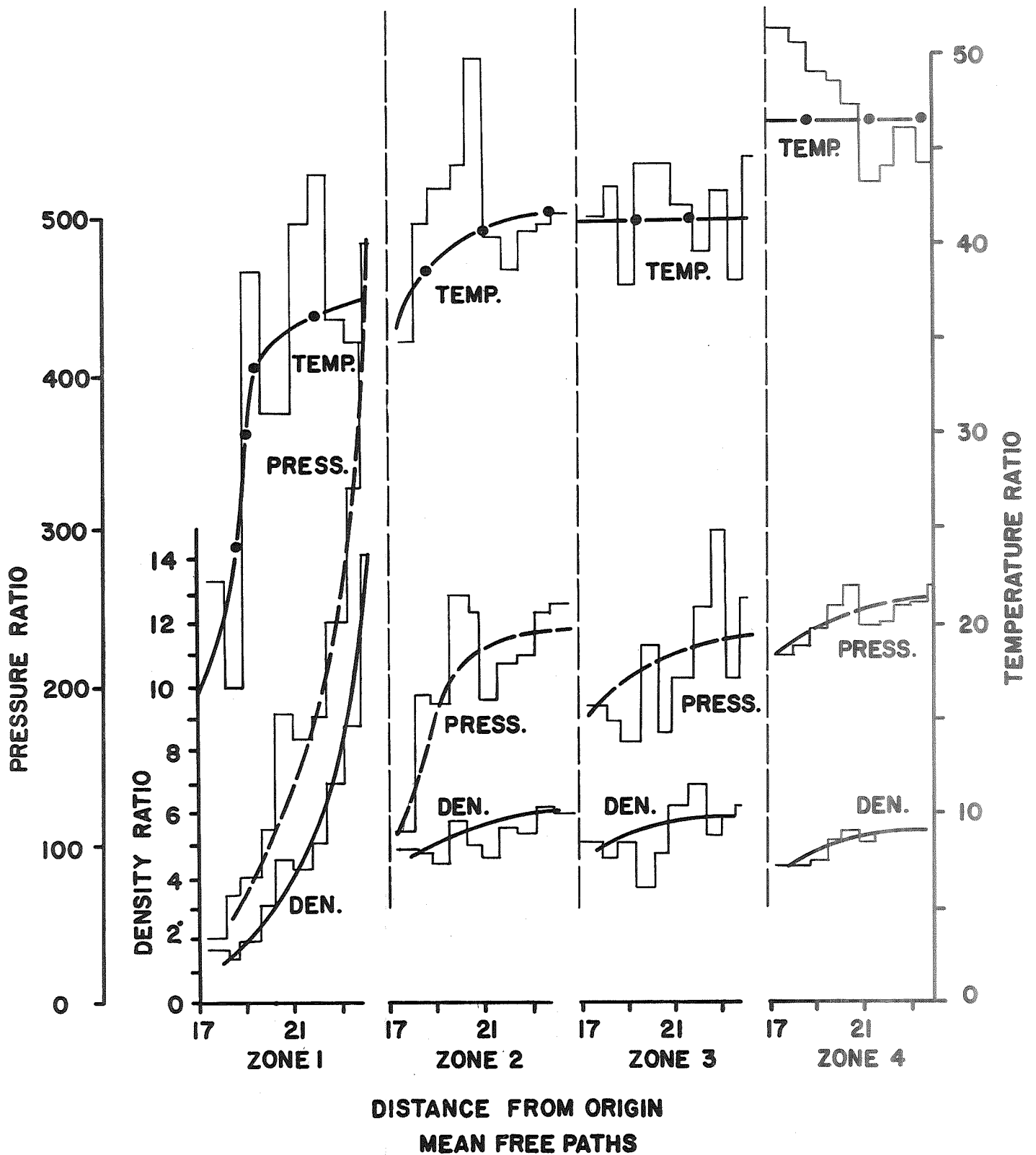
FIGURE 7: DENSITY, PRESSURE AND TEMPERATURE PROFILES OF IMPLODING
SHOCK WAVE AT TIME 0.002726/V_m sec. AFTER PISTON
COMMENCED MOVING. DIFFUSE REFLECTIVE WALL. REGIONS WHERE
4 CELLS PER SHELL FORMED. ZONE 1 ARE CELLS CLOSEST TO
WALL AND ZONE 4 IS FURTHEST FROM WALL. SEE FIGURE 2.
ORIGIN OF COORDINATES 6 MEAN FREE PATHS FROM CENTRE.
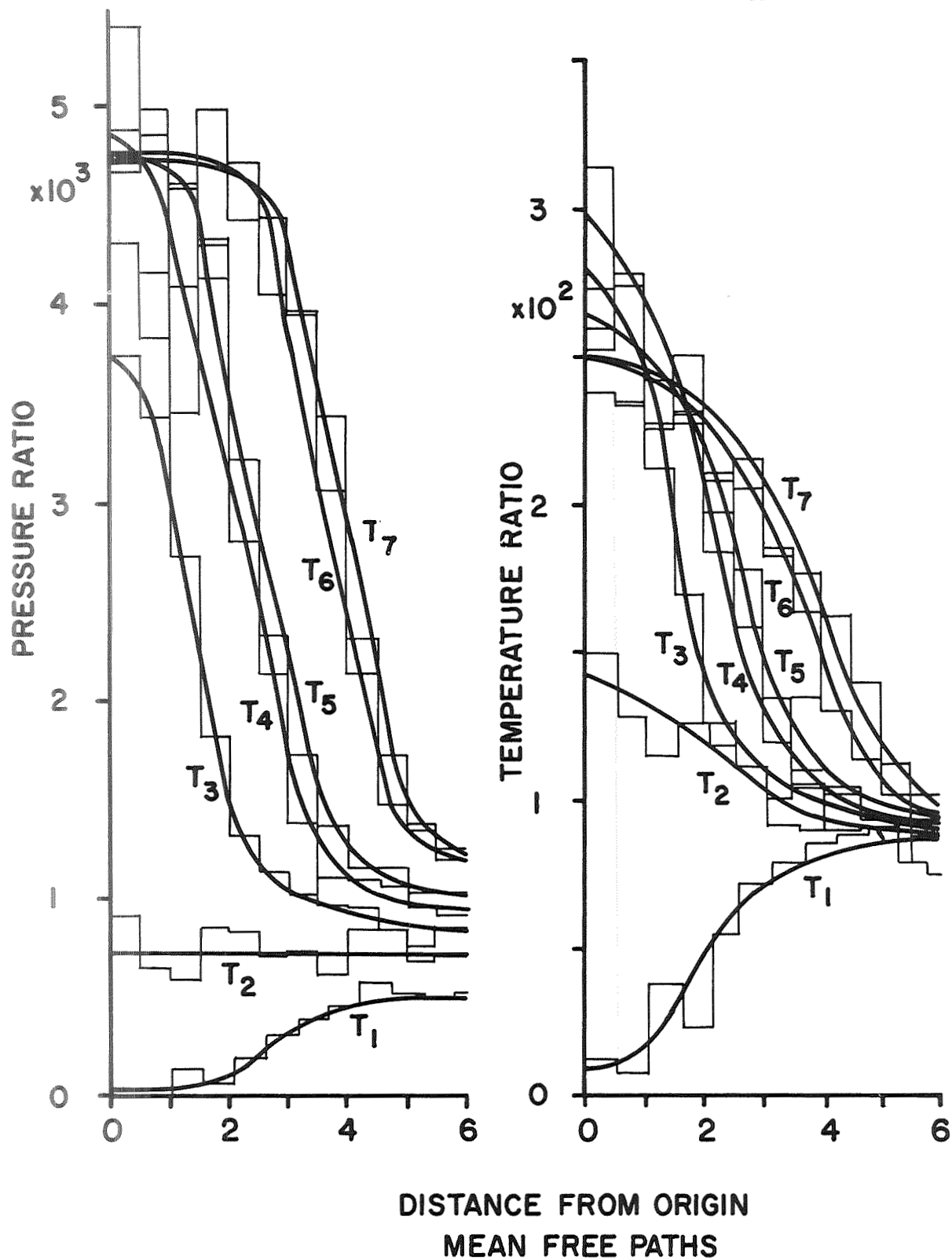
FIGURE 8: PRESSURE AND TEMPERATURE PROFILES DURING THE REFLECTION
OF A HEMISPHERICAL IMPLODING SHOCK WAVE AT VARIOUS TIMES
T. SPECULARLY REFLECTING WALL. ORIGIN OF CO-ORDINATES
6 MEAN FREE PATHS FROM CENTRE. $T_1 = 0.003801/Vm$ SEC,
$T_2 = 0.003946/Vm$ SEC, $T_3 = 0.004087/Vm$ SEC, $T_4 = 0.004207/Vm$ SEC, $T_5 = 0.004291/Vm$ SEC, $T_6 = 0.004404/Vm$ SEC,
$T_7 = 0.00486/Vm$ SEC.
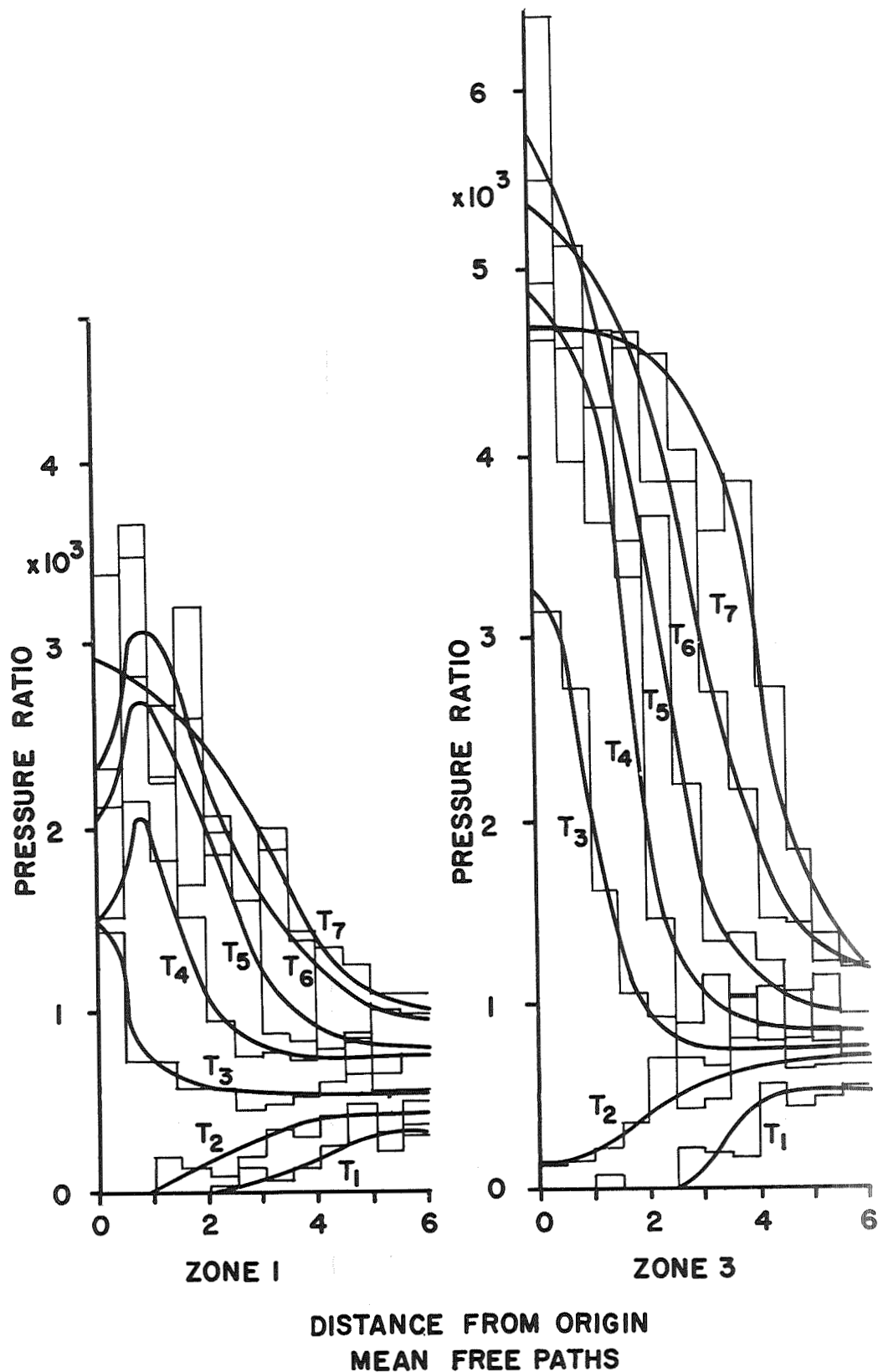
FIGURE 9: PRESSURE PROFILES DURING THE REFLECTION OF A HEMISPHERICAL IMPLODING SHOCK WAVE AT VARIOUS TIME T. DIFFUSE REFLECTING WALL. ORIGIN OF CO-ORDINATES 6 MEAN FREE PATHS FROM CENTRE.
$T_1 = 0.003795/Vm$ SEC, $T_2 = 0.003936/Vm$ SEC, $T_3 = 0.004081/Vm$ SEC, $T_4 = 0.004204/Vm$ SEC, $T_5 = 0.004298/Vm$ SEC, $T_6 = 0.0044/Vm$ SEC, $T_7 = 0.004501/Vm$ SEC.
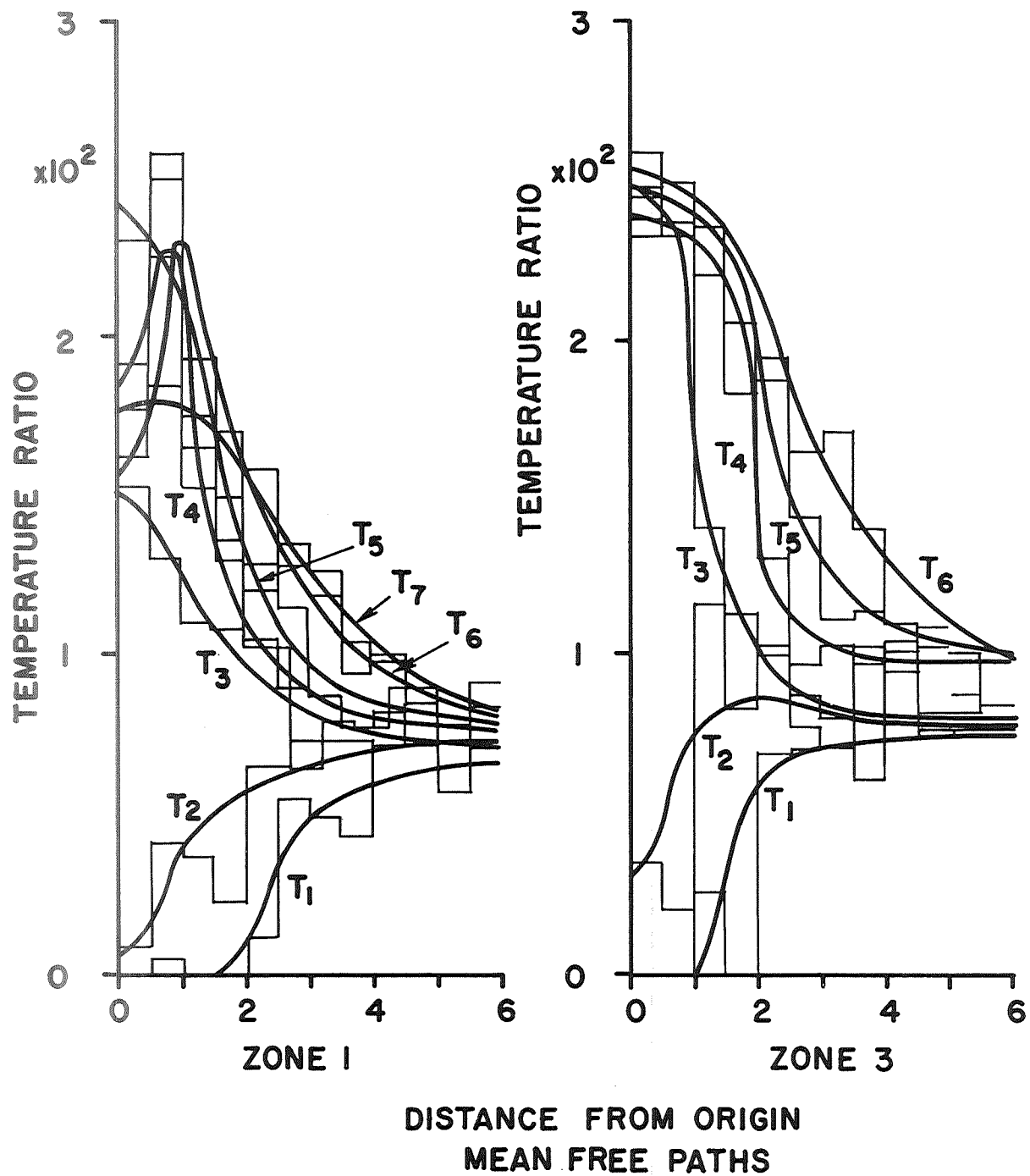
FIGURE 10: TEMPERATURE PROFILES DURING THE REFLECTION OF A HEMIS-
PHERICAL IMPLODING SHOCK WAVE AT VARIOUS TIMES T.
DIFFUSE REFLECTING WALL. SEE FIG.7 FOR DETAILS
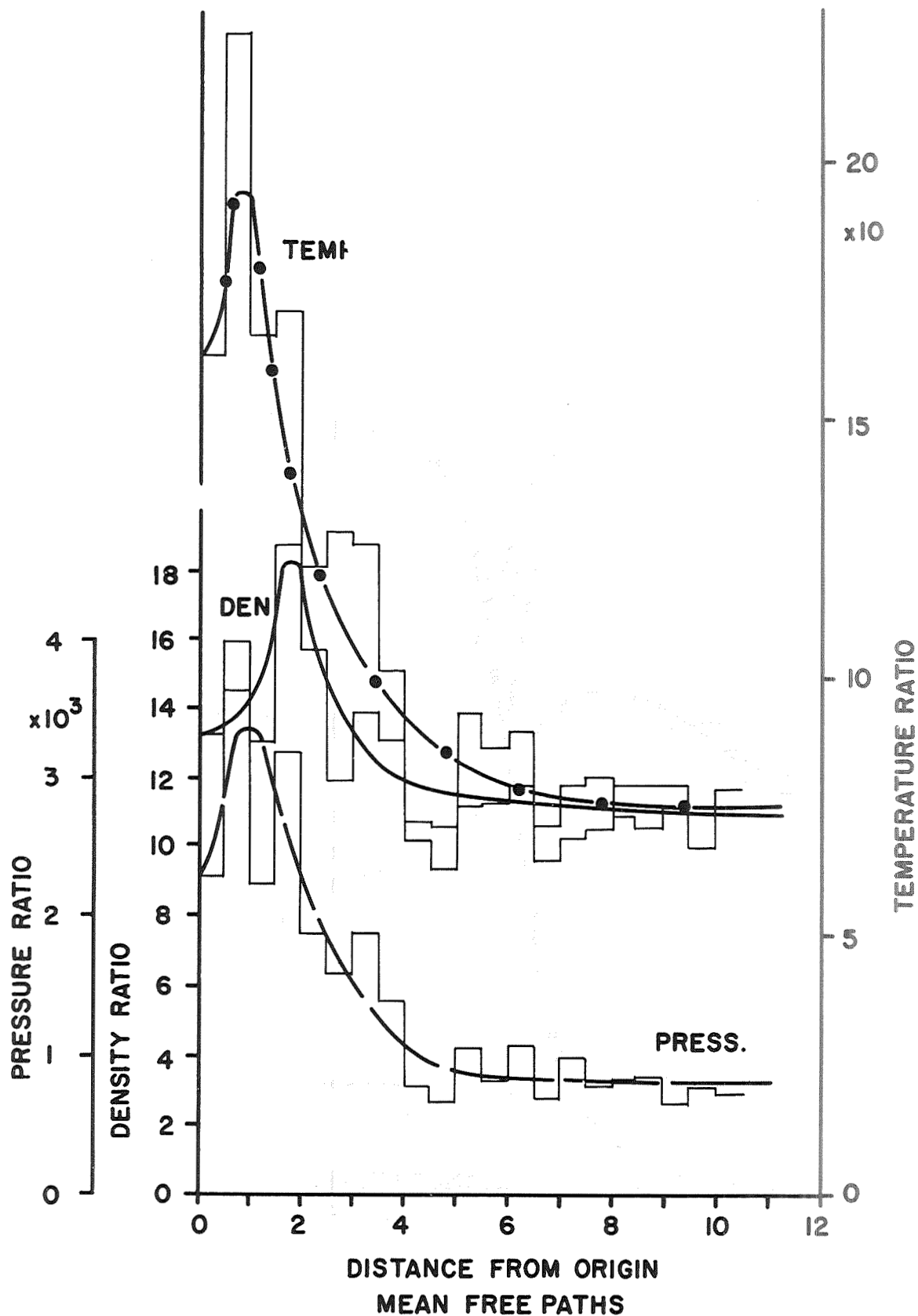
FIGURE 11: DENSITY, PRESSURE AND TEMPERATURE PROFILES FOR CELLS Z_{1j}
AT TIME 0.0044/Vm SEC. AFTER PISTON COMMENCED GENERATION
OF IMPLODING SHOCK. DIFFUSE REFLECTIVE WALL. REGION
WHERE ONLY 3 CELLS PER SHELL FORMED. ORIGIN OF CO-
ORDINATES 6 MEAN FREE PATHS FROM CENTRE.
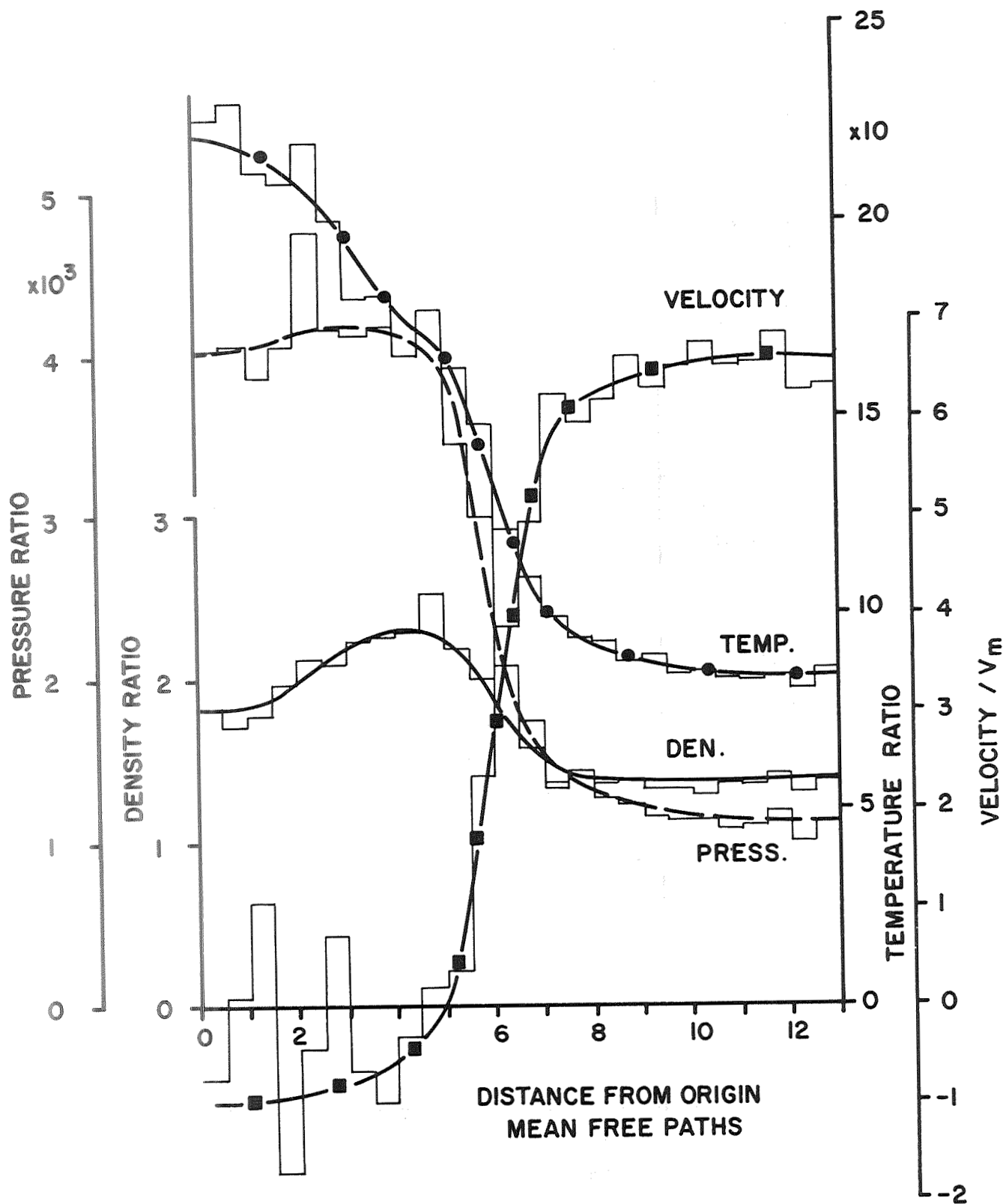
FIGURE 12: DENSITY, PRESSURE, VELOCITY AND TEMPERATURE PROFILES AS IN FIG.3 AT TIME 0.004639/Vm SEC.

FIGURE 13: DENSITY, PRESSURE, TEMPERATURE AND VELOCITY PROFILES OF
IMPLODING SHOCK WAVE AT TIME $0.004624/V_m$ SEC. AFTER
PISTON COMMENCED MOVING. DIFFUSE REFLECTIVE WALL. ORIGIN
OF CO-ORDINATES 6 MEAN FREE PATHS FROM CENTRE REGION WHERE
ONLY 3 CELLS PER SHELL WERE FORMED Z_{1j}, FIG.2

FIGURE 14: DENSITY, PRESSURE OF TEMPERATURE PROFILES OF IMPLODING SHOCK
WAVE AT TIME 0.004624/Vm SEC. AFTER PISTON COMMENCED MOVING.
DIFFUSE REFLECTIVE WALL. REGION WHERE ONLY 3 CELLS PER SHELL
WERE FORMED Z_{2j}, FIG.2.
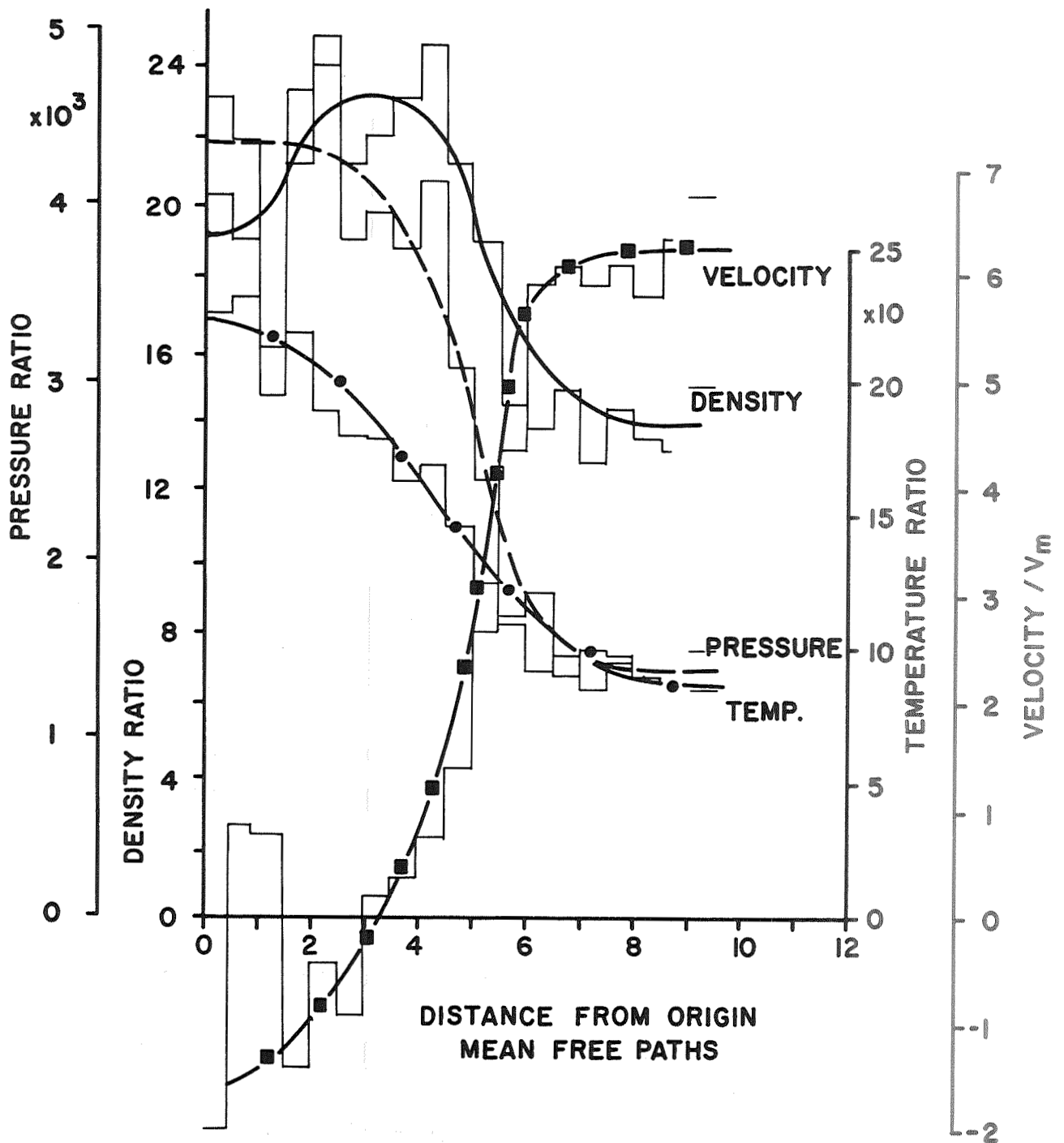
FIGURE 15: DENSITY, PRESSURE, TEMPERATURE AND VELOCITY PROFILES AS
IN FIG.13 FOR CELL Z_{3j}
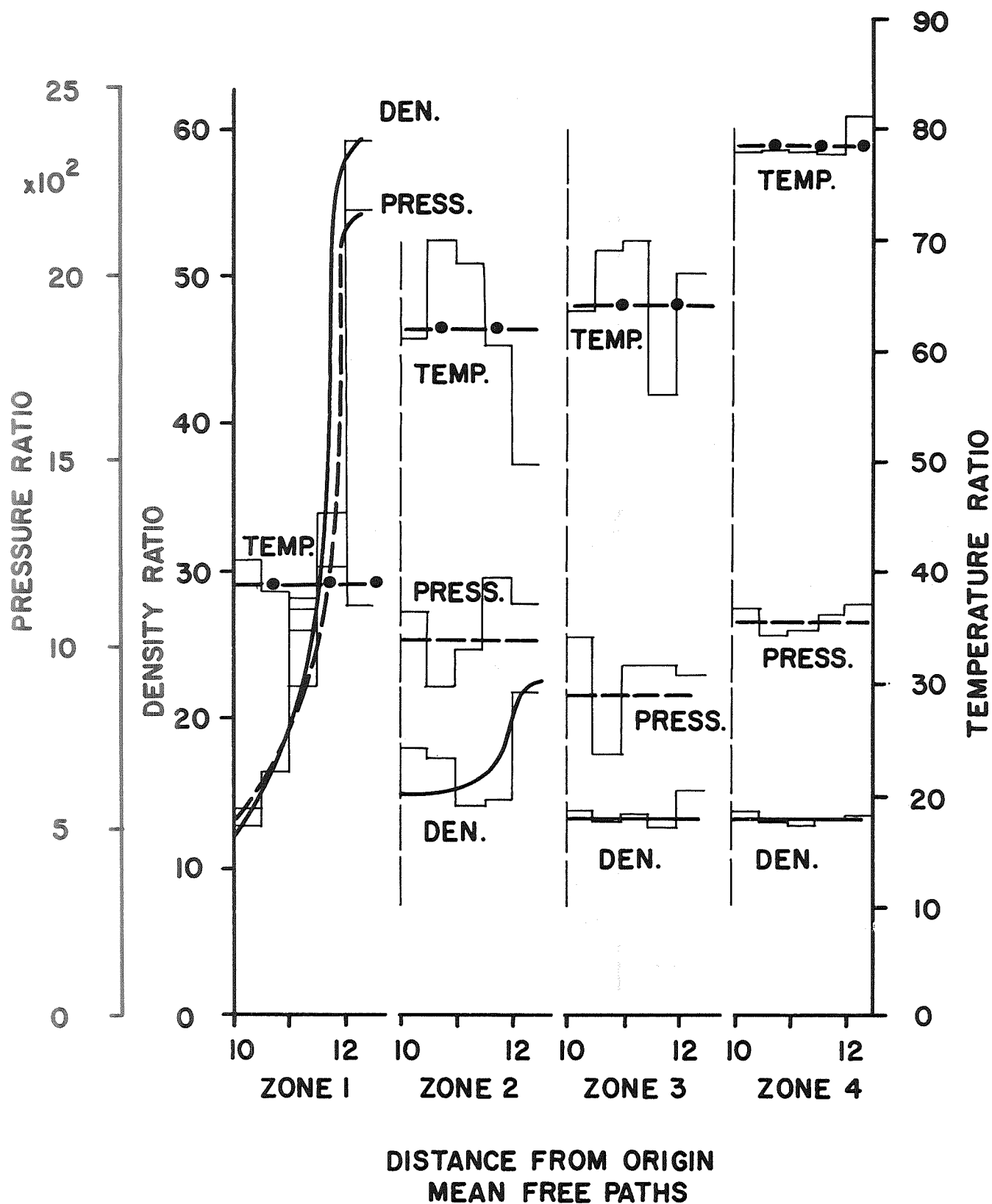
FIGURE 16: DENSITY, PRESSURE AND TEMPERATURE PROFILES OF IMPLODING SHOCK CONDITIONS AS IN FIG.13. REGION WAVE 4 CELLS/SHELL FORMED.
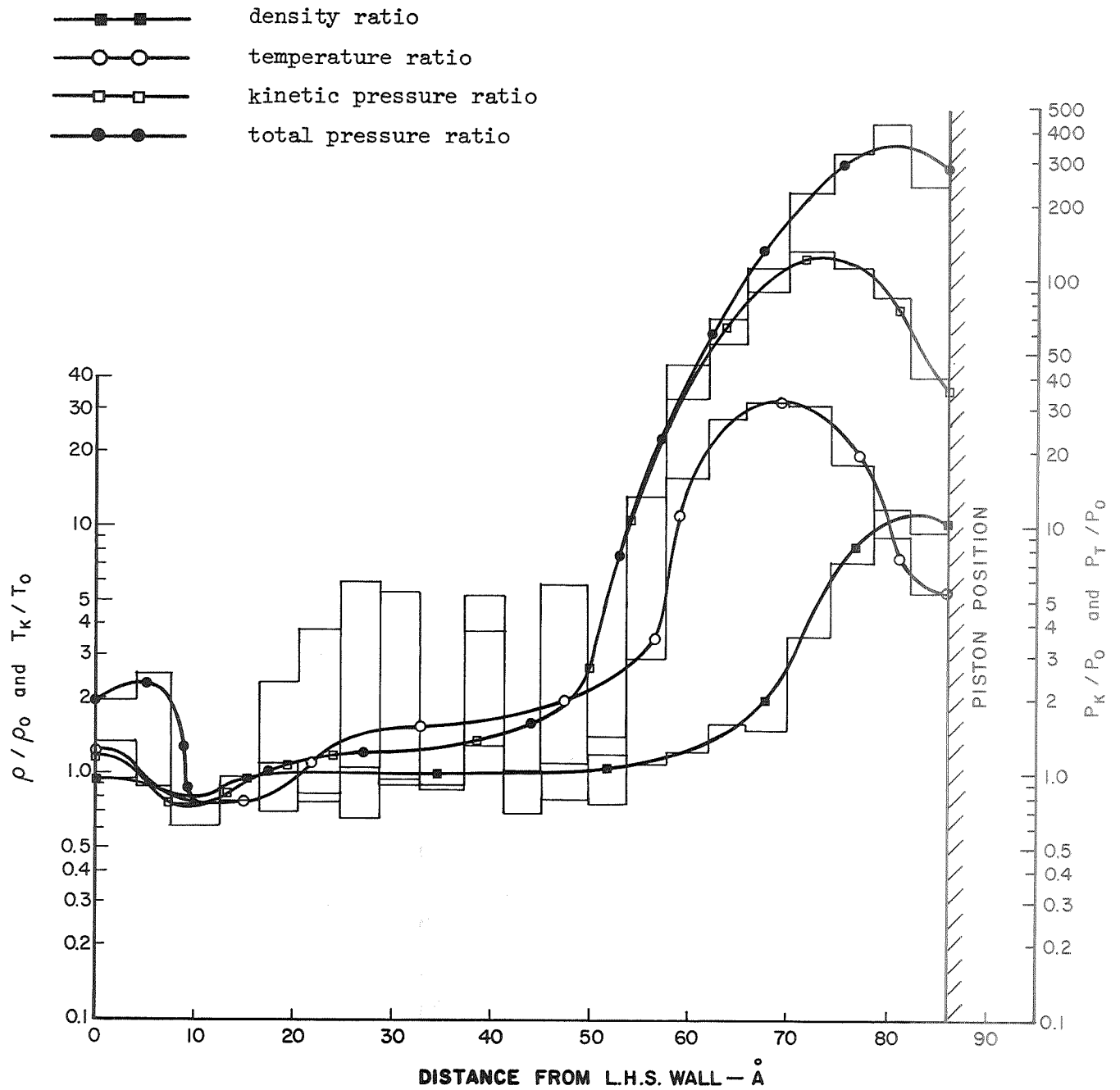
Fig.17 Shock wave generation by a tungsten piston moving into argon with initial number density .245 x 10^{22}. Piston velocity .293 x 10^6 cm/sec.

a) Time 0.199 x 10^{-11} sec after piston started moving
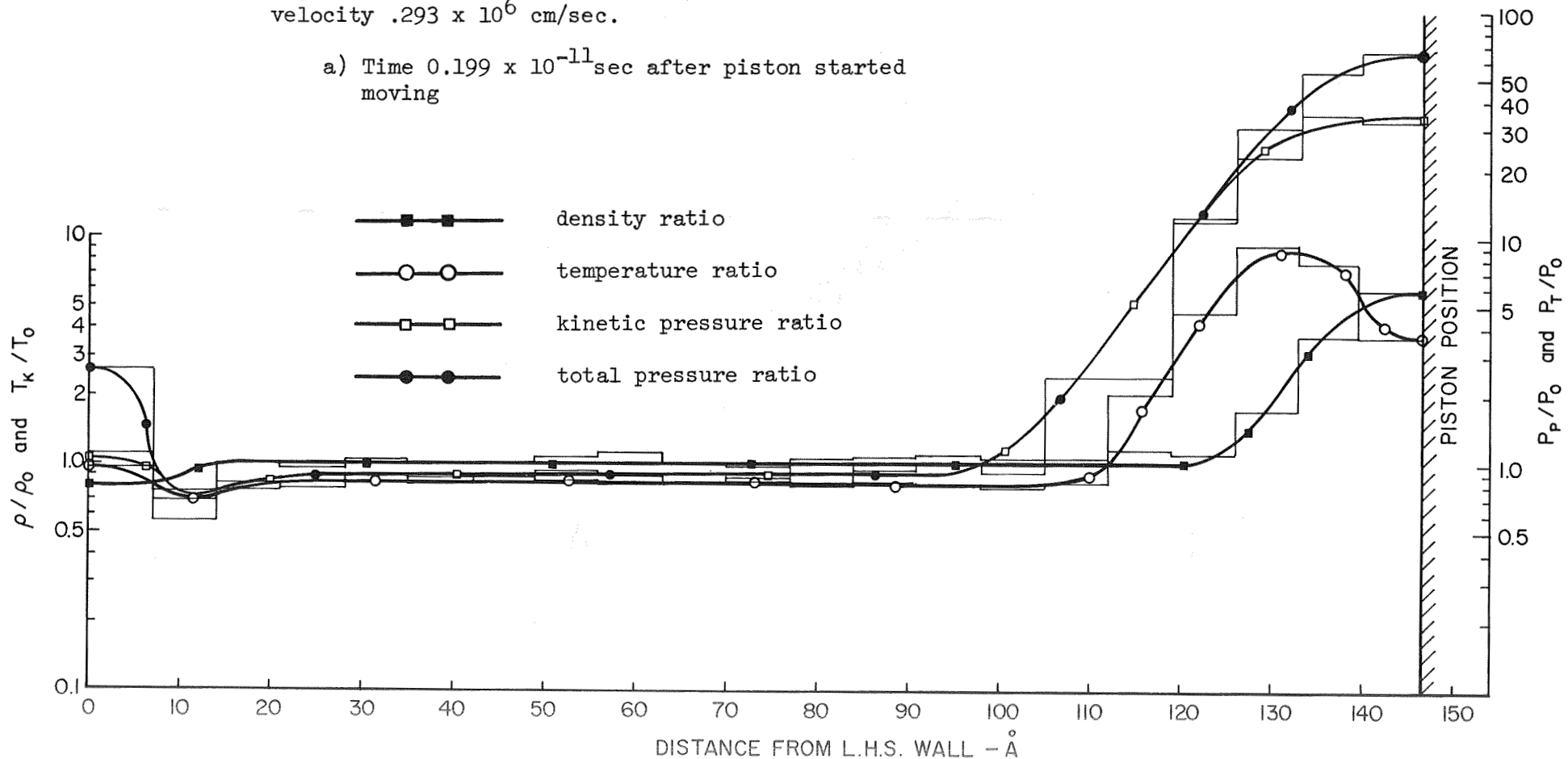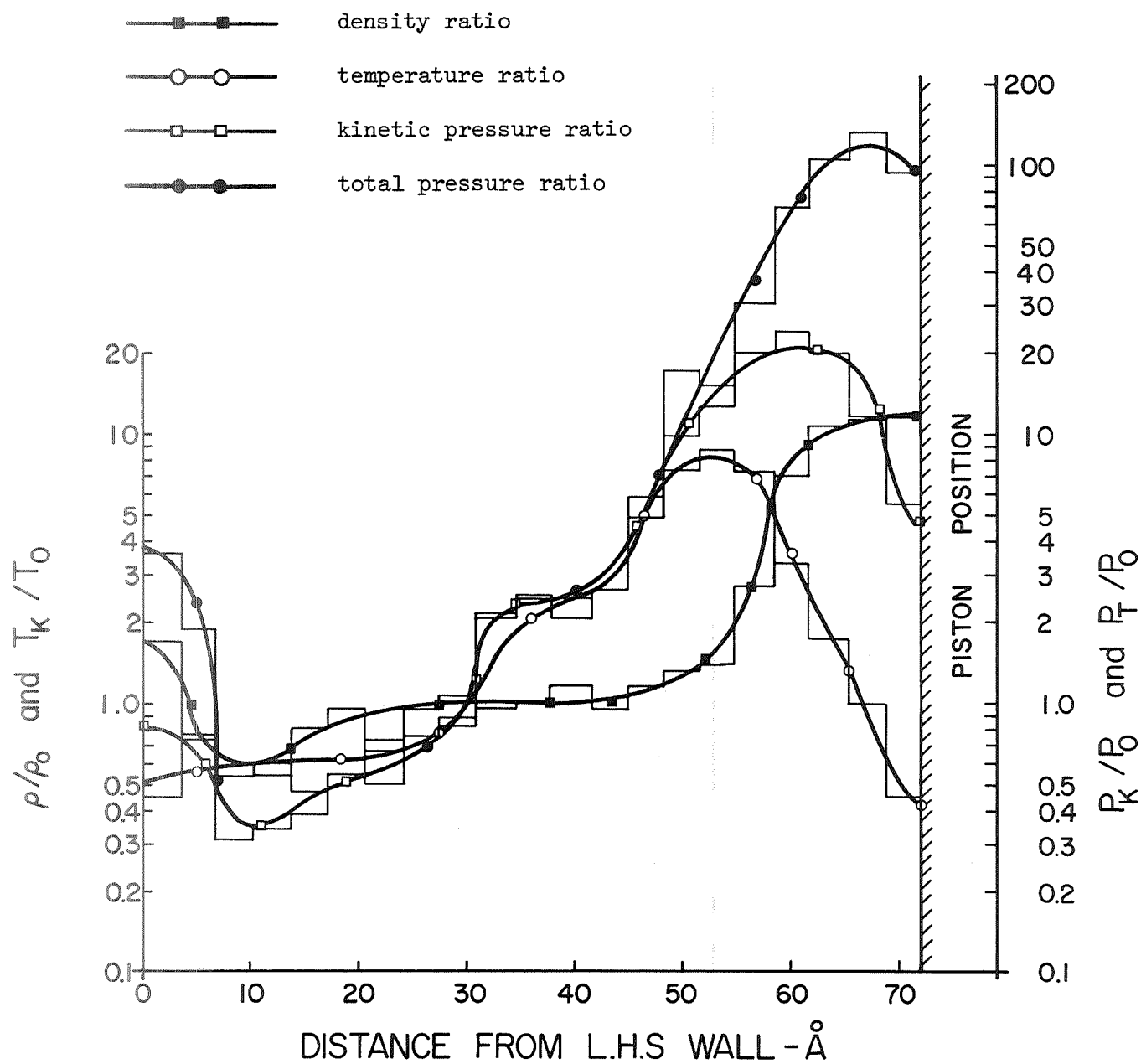
Fig.17   b) Time 0.449 x 10^{-11} sec after piston started
          moving
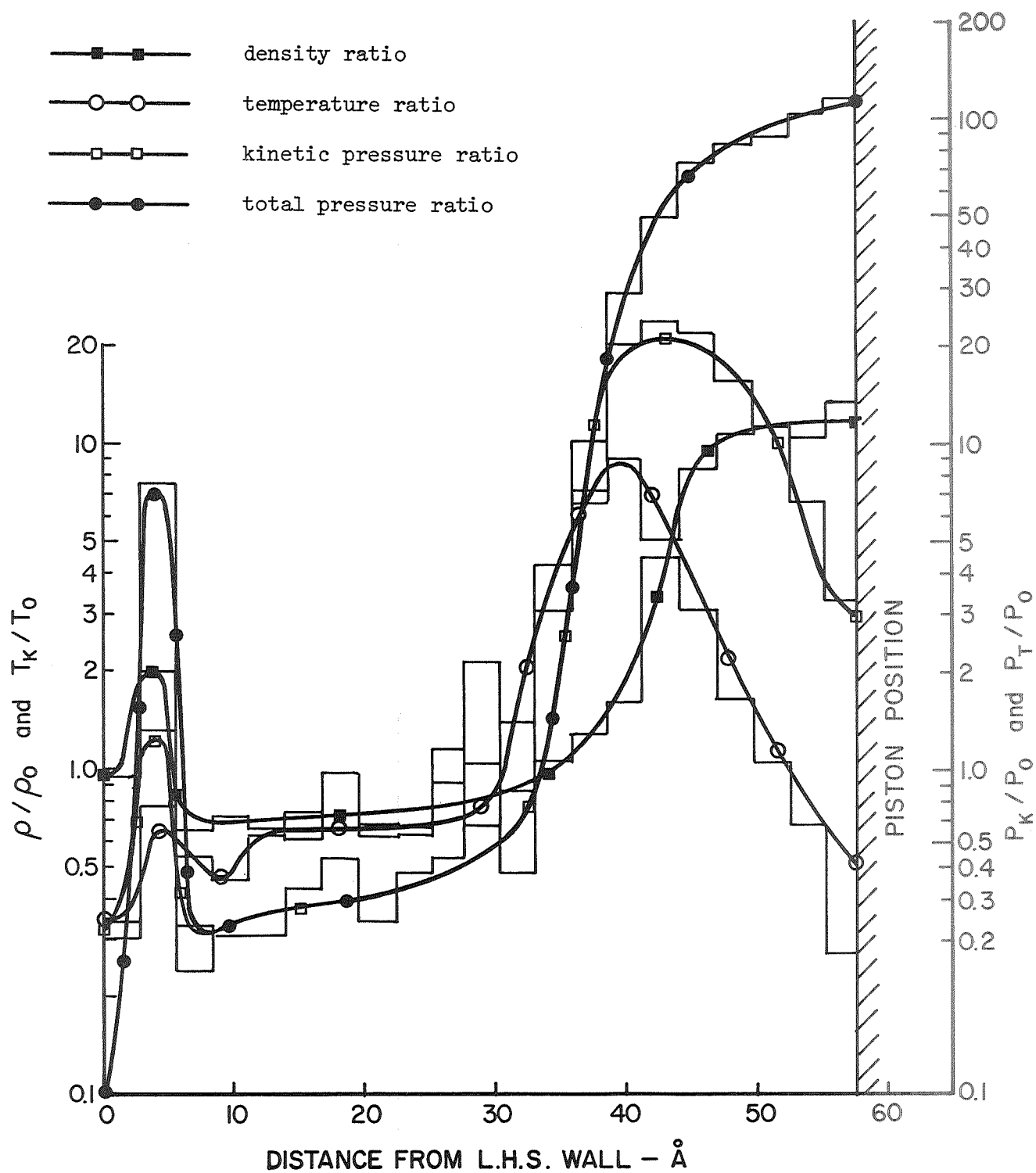
Fig.17   c) Time 0.4986×10^{-11} sec after piston started moving
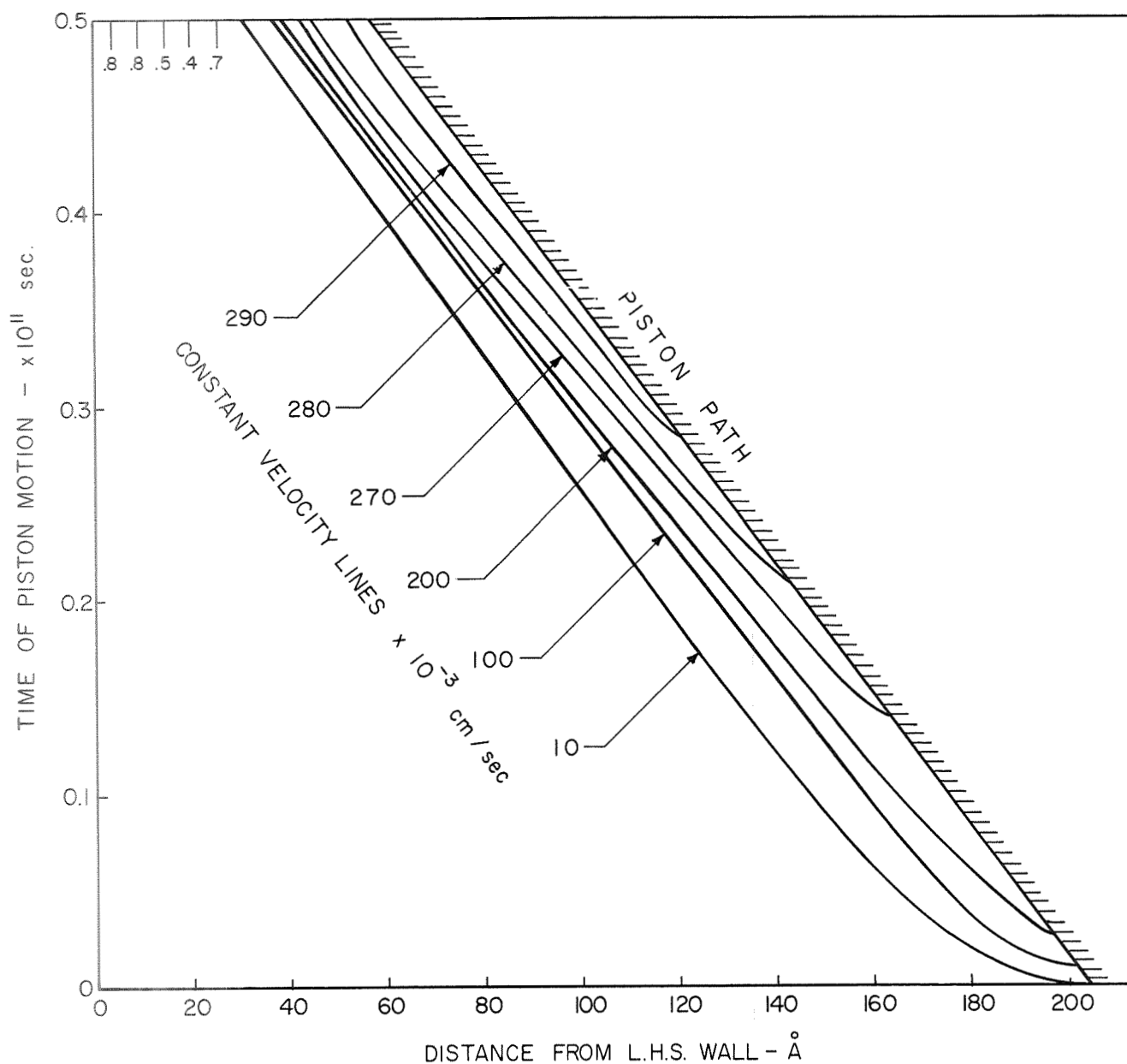
Fig.18 **Approximate curves** of constant mass velocity behind
shock wave generated in Argon initial density
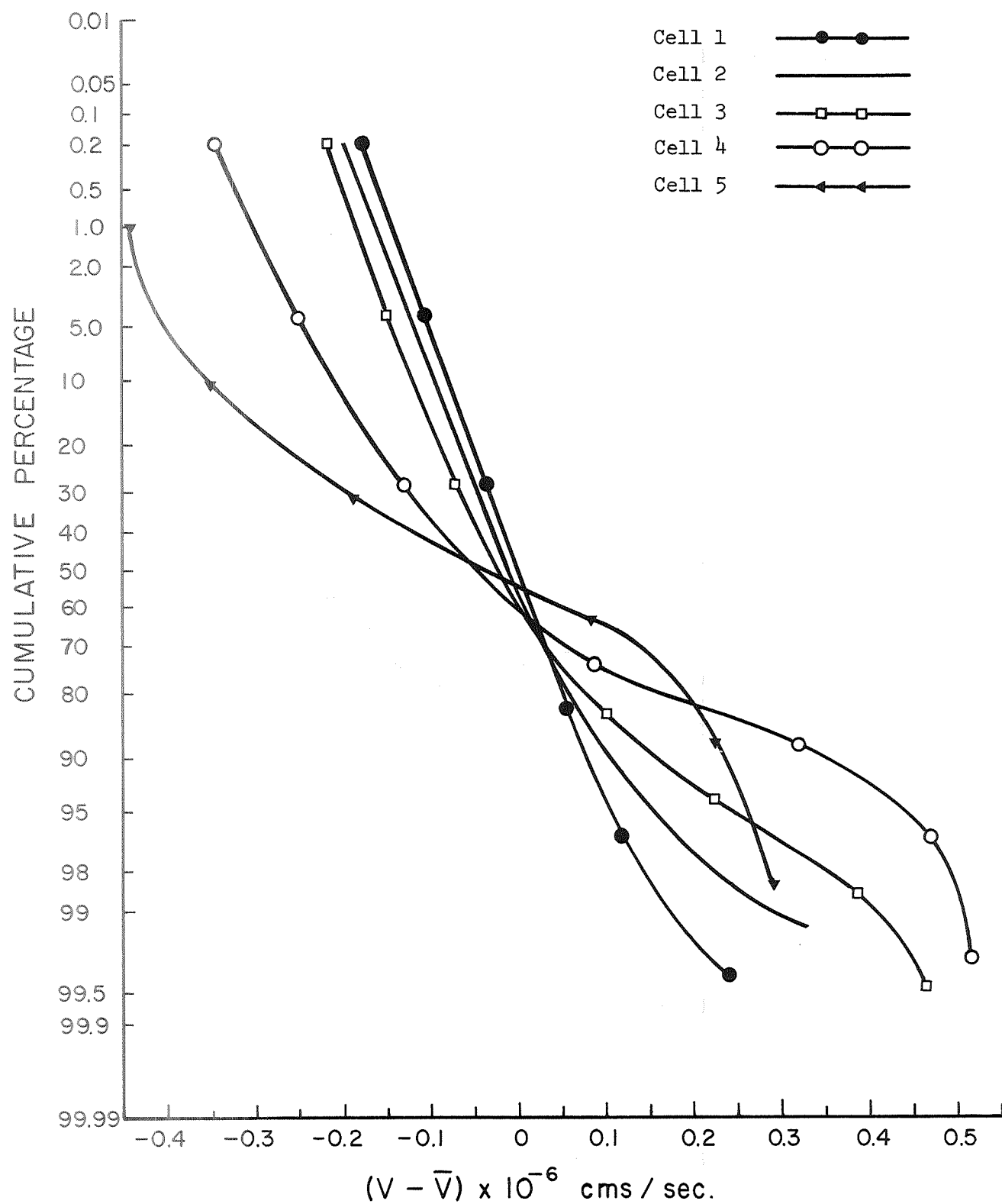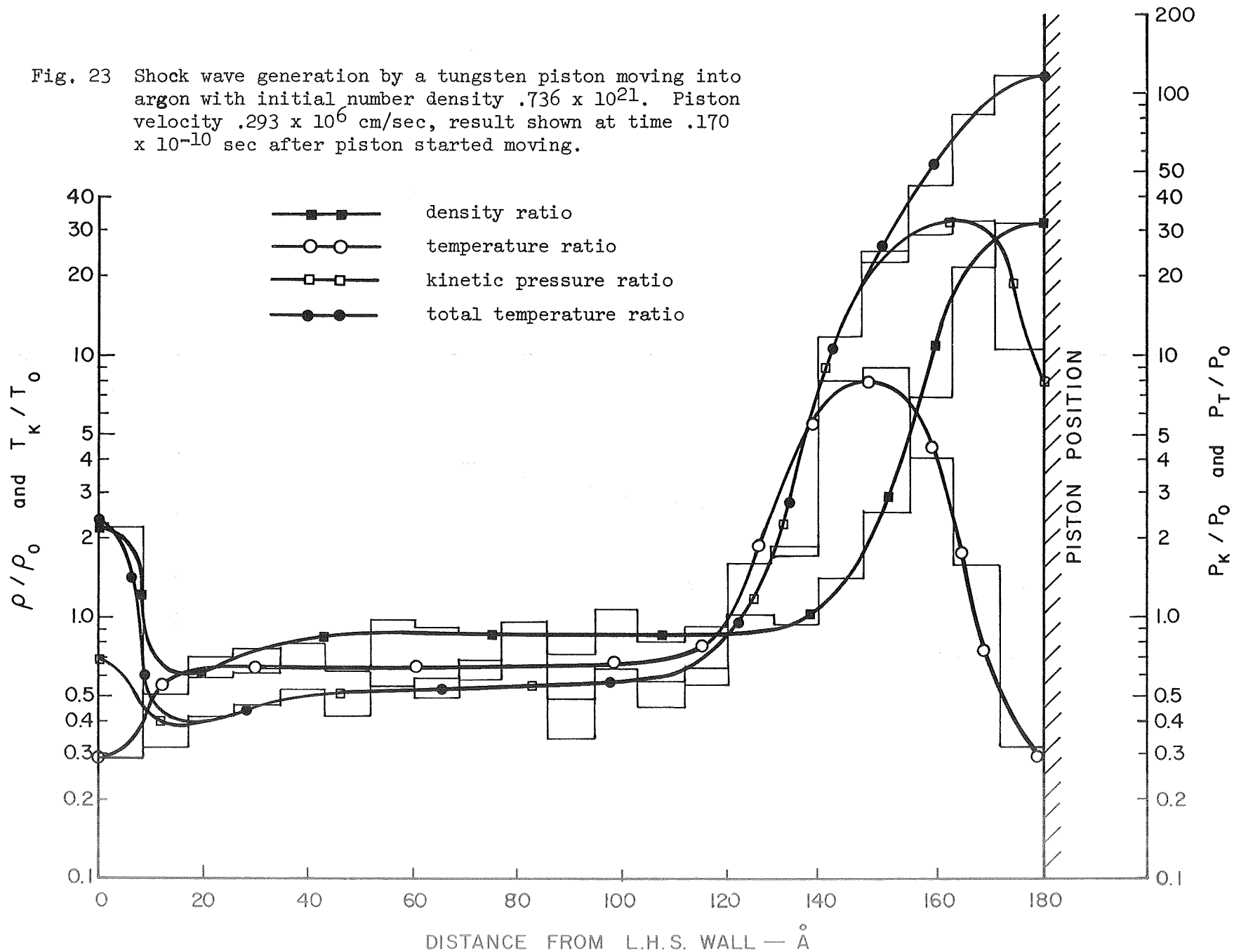.245 x 10^{22} number density, piston velocity
.293 x 10^6 cm/sec.

Fig.19 Longitudinal velocity distributions integrated across both lateral velocity distributions under conditions specified for figure 17c. Numbering the cells shown in figure 2c as 1 next to the piston
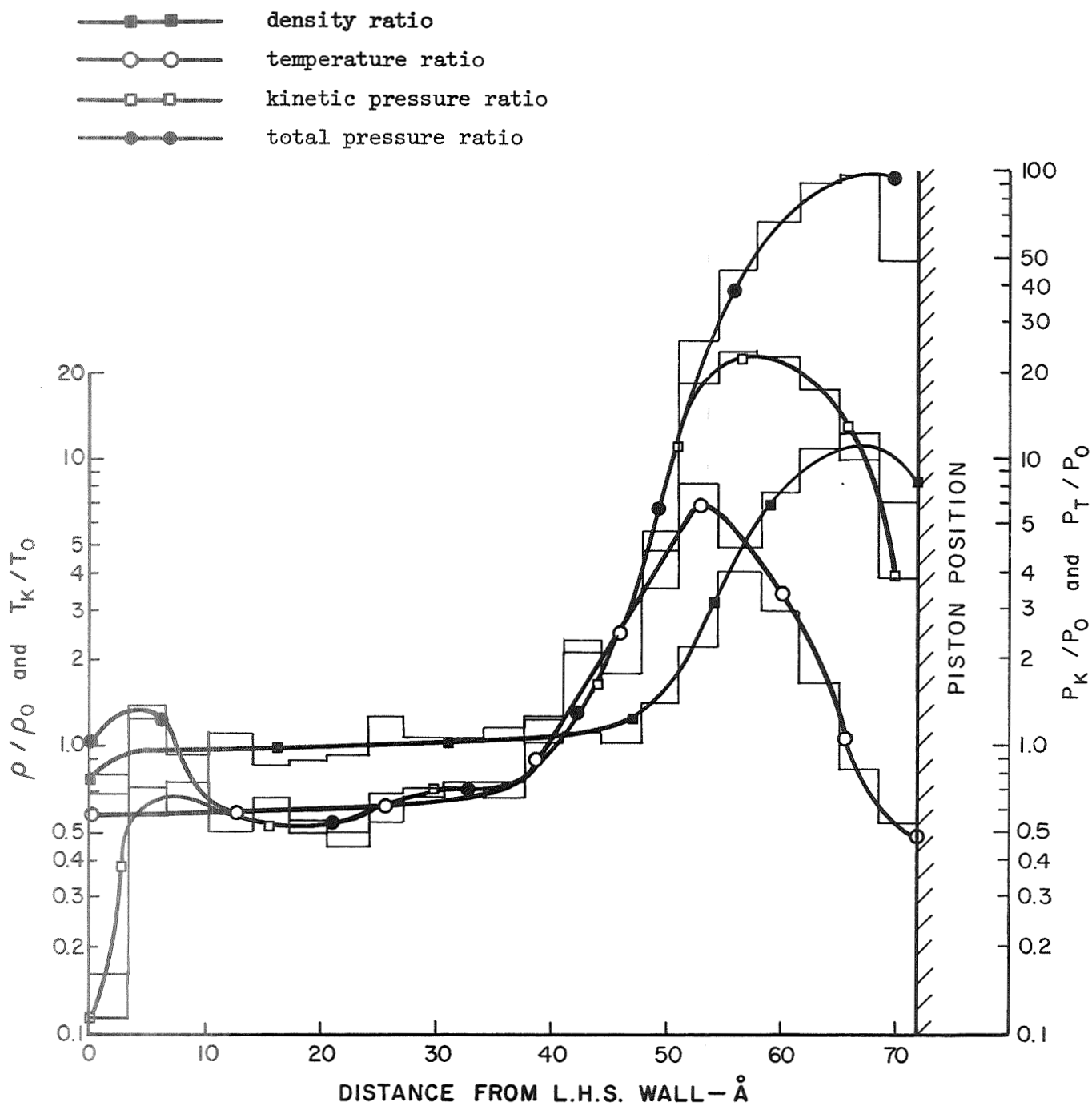
Fig.20 **Shock wave generation** by a dense argon piston moving into argon with initial number density .245 x 10^{22}. Piston velocity .293 x 10^6 cm/sec, result shown at time .449 x 10^{-11} sec after piston started moving.

Fig.21 Shock wave generation by a tungsten piston moving into argon with initial number density .245 x 10^{22}. Piston velocity .586 x 10^{6} cm/sec, result shown at time .198 x 10^{-11} sec after piston started moving.
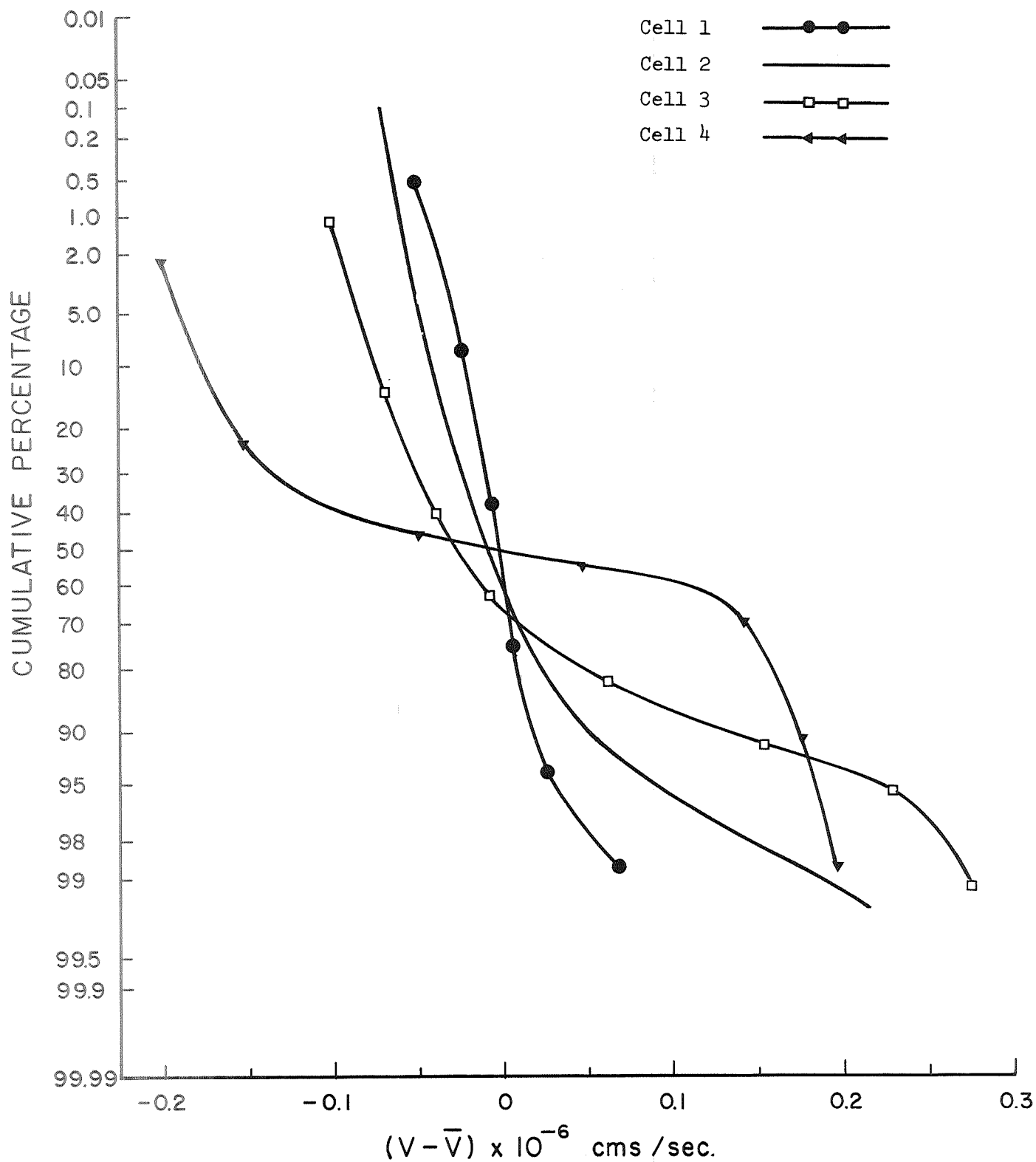
Fig. 22 Longitudinal velocity distributions integrated across
both lateral velocity distributions under conditions
specified for figure 21. Numbering the cells shown
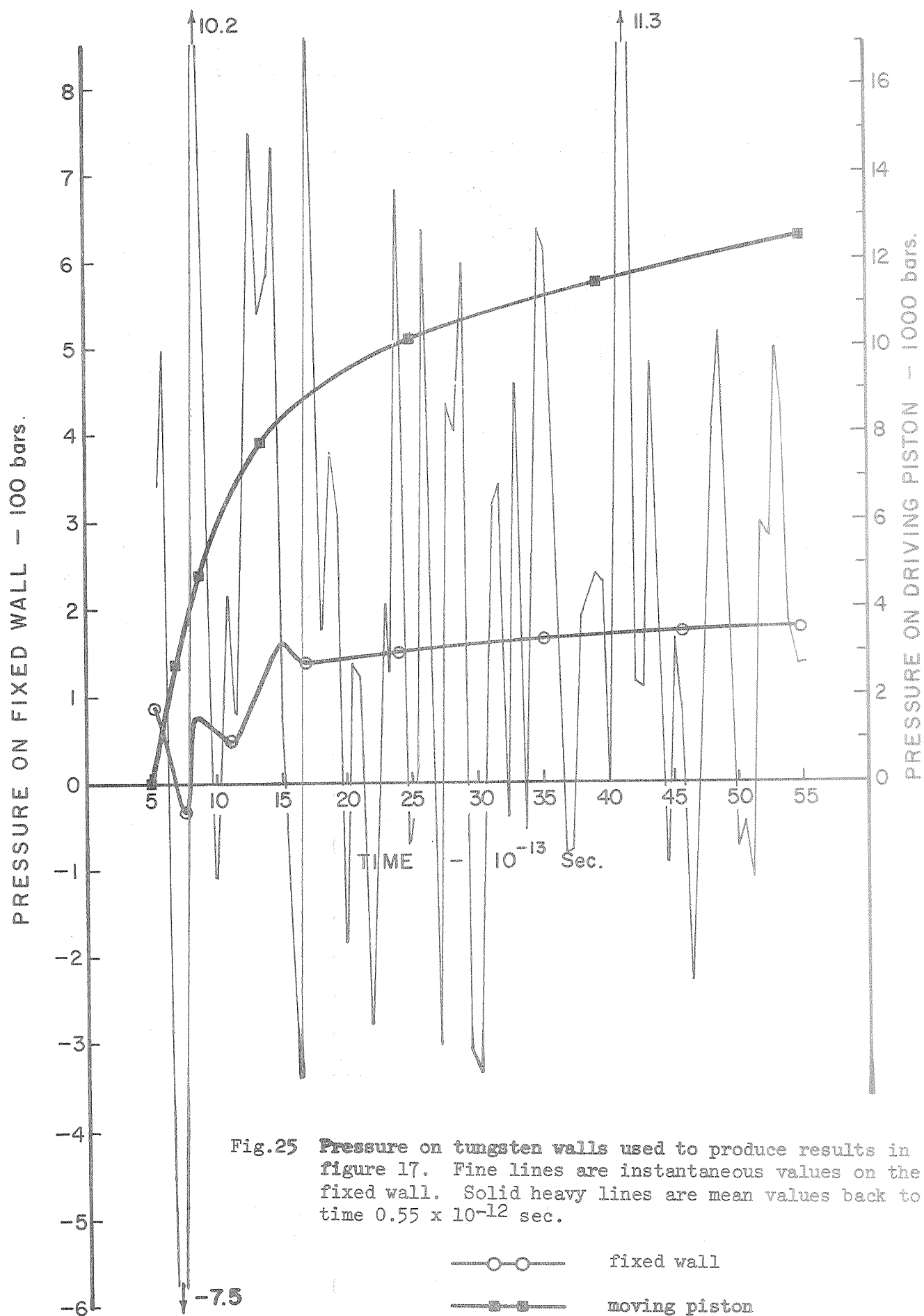in figure 21 as 1 next to the piston.

Fig. 23 Shock wave generation by a tungsten piston moving into argon with initial number density $.736 \times 10^{21}$. Piston velocity $.293 \times 10^6$ cm/sec, result shown at time $.170 \times 10^{-10}$ sec after piston started moving.

Fig. 24 Longitudinal velocity distributions integrated across
both lateral velocity distributions under conditions
specified for figure 23. Numbering cells shown in
figure 23 as 1 next to the piston.

Fig.25 Pressure on tungsten walls used to produce results in figure 17. Fine lines are instantaneous values on the fixed wall. Solid heavy lines are mean values back to time 0.55 x 10⁻¹² sec.

———O——O——— fixed wall

———■——■——— moving piston

Fig.26 Shock wave generation by an imploding spherical dense argon piston moving into argon with initial number density .245 x 10^{22}. Piston velocity .293 x 10^6cm/sec, results shown at various times after piston commenced moving. Centre is occupied by a sphere of radius 19.4 Å.

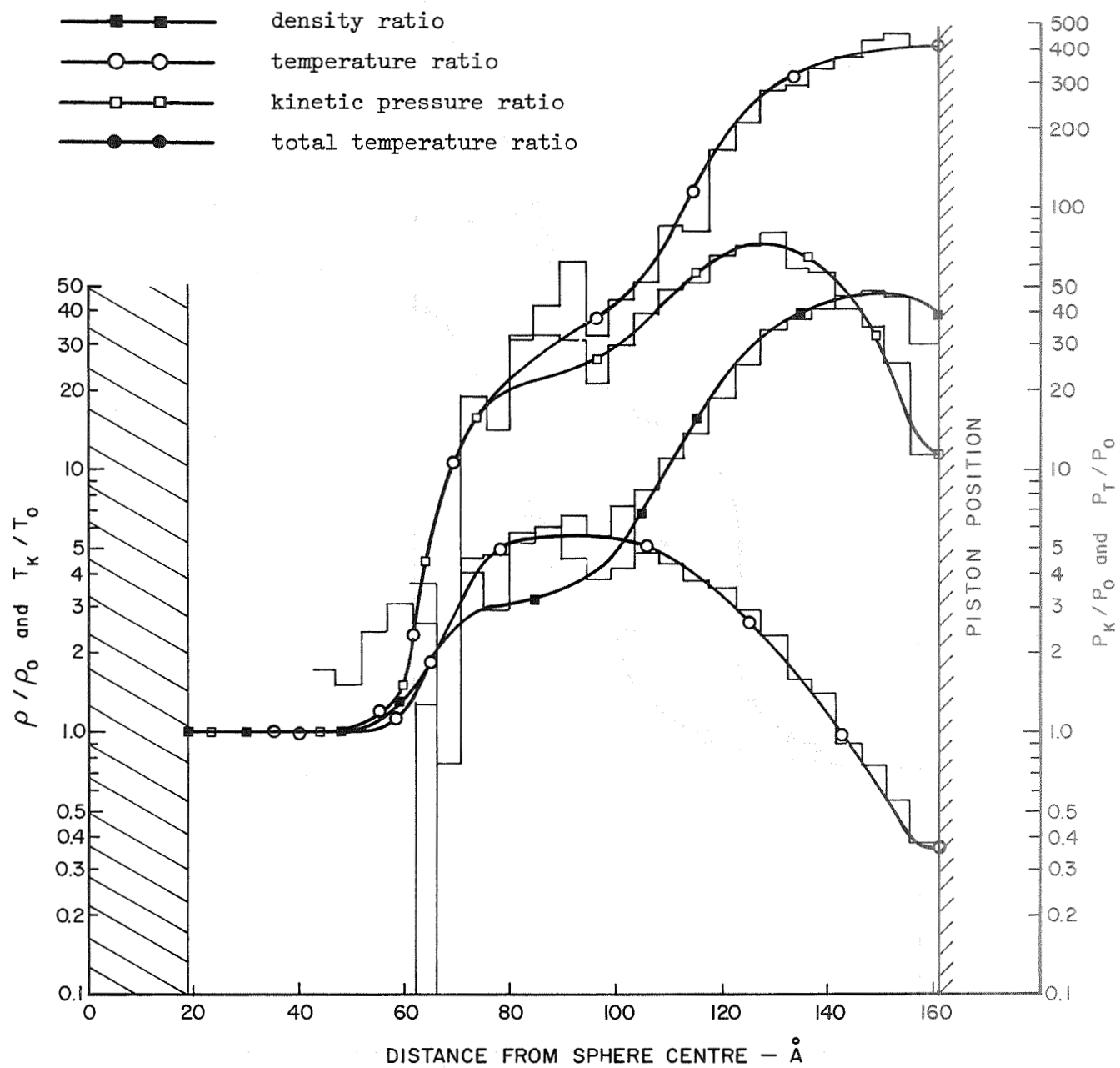a) 0.672 x 10^{-11} sec after piston started moving
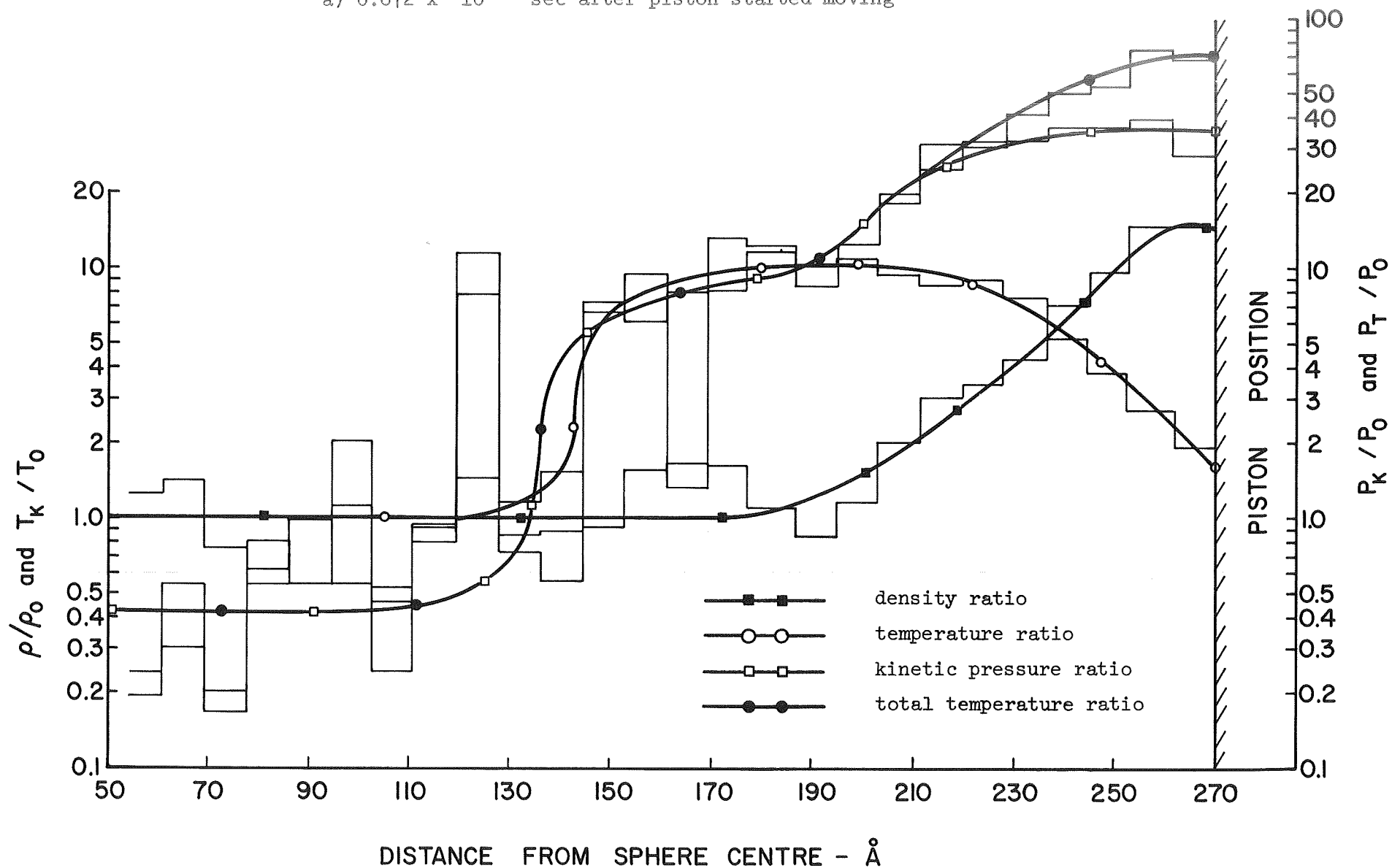
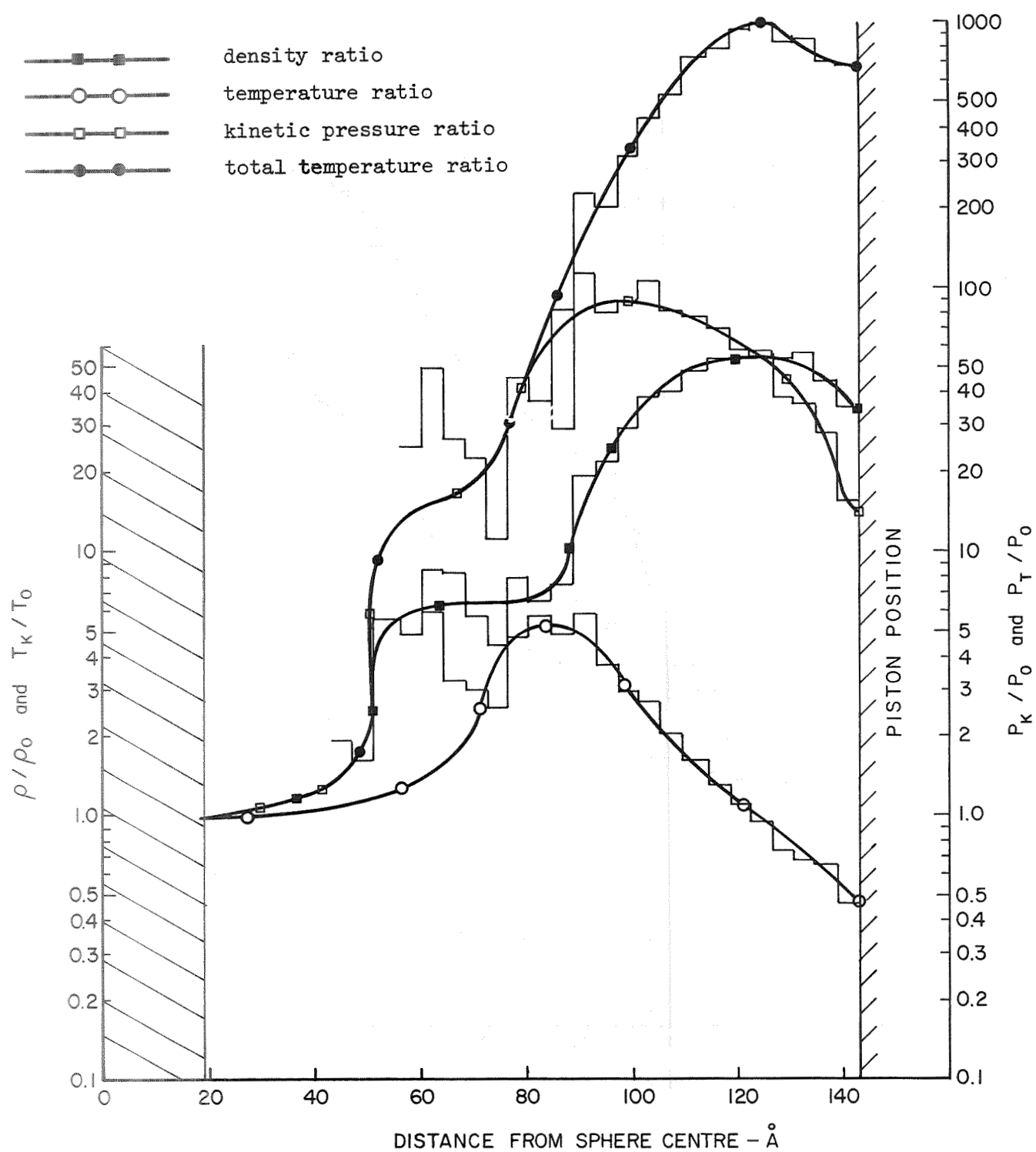Fig. 26 b) 1.045×10^{-11}sec after piston started moving

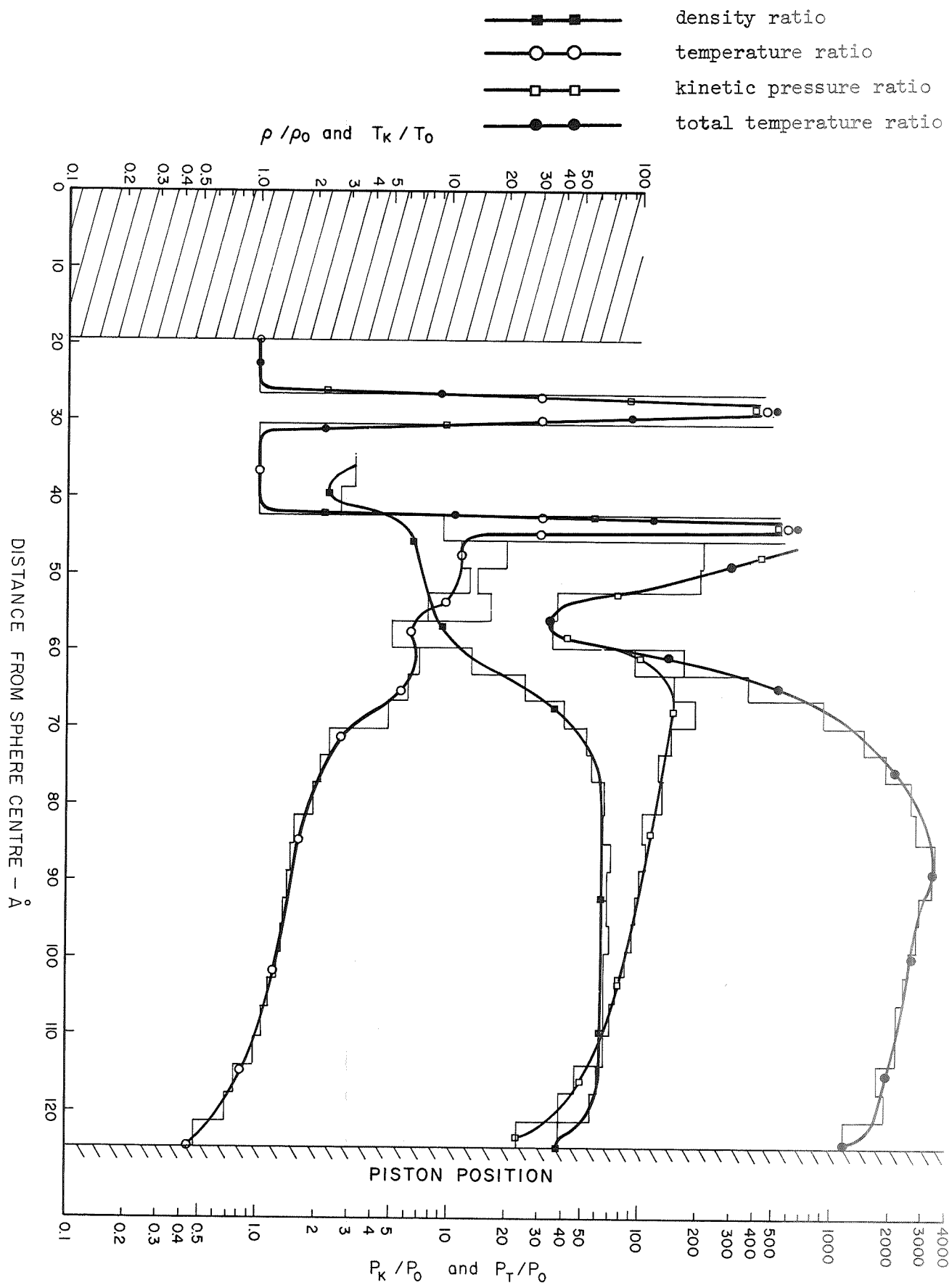Fig. 26 c) 1.105×10^{-11} sec after piston started moving

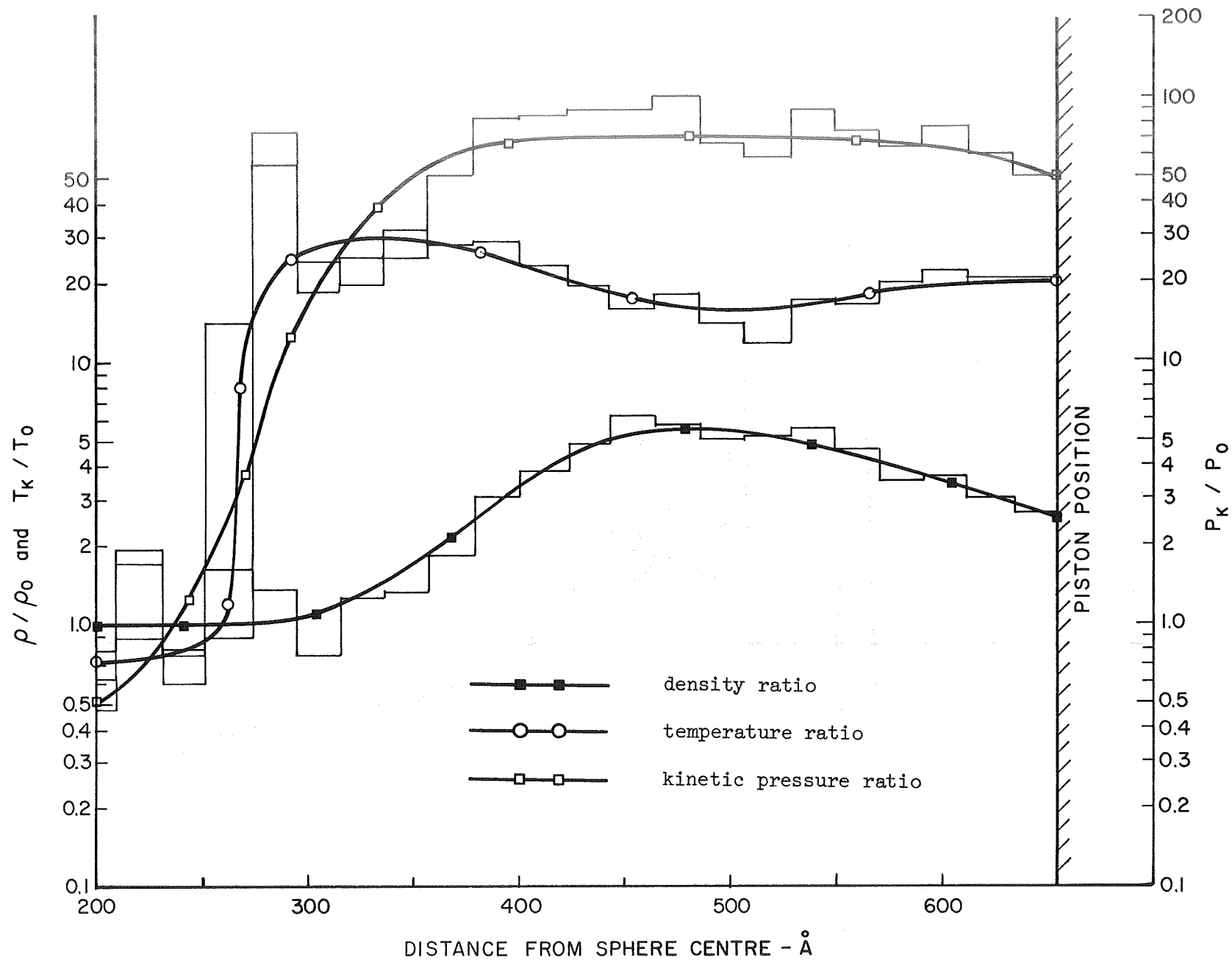Fig. 26 d) 1.165×10^{-11} sec after piston started moving

Fig. 27 Shock wave generation by an imploding spherical dense
argon piston moving into argon with initial pressure
3 atmospheres. Piston velocity .293 x 10⁶ cm/sec.